

# **WZA: A window-based method for characterizing genotype-environment association**

Tom R. Booker<sup>1,2,3,\*</sup>, Sam Yeaman<sup>1</sup>, Michael C. Whitlock<sup>2,3</sup>

1. Department of Biological Sciences, University of Calgary, Calgary, Canada

2. Department of Zoology, University of British Columbia, Vancouver, Canada

3. Biodiversity Research Centre, University of British Columbia, Vancouver, Canada

\*Corresponding author: [booker@zoology.ubc.ca](mailto:booker@zoology.ubc.ca)

## Abstract

Genotype environment association (GEA) studies have the potential to elucidate the genetic basis of local adaptation in natural populations. Specifically, GEA approaches look for a correlation between allele frequencies and putatively selective features of the environment. Genetic markers with extreme evidence of correlation with the environment are presumed to be tagging the location of alleles that contribute to local adaptation. In this study, we propose a new method for GEA studies called the weighted-Z analysis (WZA) that combines information from closely linked sites into analysis windows in a way that was inspired by methods for calculating  $F_{ST}$ . We analyze simulations modelling local adaptation to heterogeneous environments either using a GEA method that controls for population structure or an uncorrected approach. In the majority of cases we tested, the WZA either outperformed single-SNP based approaches or performed similarly. The WZA outperformed individual SNP approaches when the measured environment is not perfectly correlated with the true selection pressure or when a small number of individuals or demes was sampled. We apply the WZA to previously published data from lodgepole pine identified candidate loci that were not found in the original study.

KEYWORDS: Local adaptation, population genetics, landscape genomics

## Introduction

Studying local adaptation can provide a window into the process of evolution, yielding insights about the nature of evolvability, constraints to diversification, and the how the interplay between a species and its environment shapes its genome (e.g. Savolainen 2013). Understanding local adaptation can also benefit practical applications such as in forestry where many species of economic interest exhibit pronounced trade-offs in fitness across environments. Characterizing such trade-offs may help identify alleles involved in local adaptation, revealing candidate genes important for breeding or informing conservation management programs for buffering against the consequences of anthropogenic climate change (Aitken and Whitlock 2013). Whatever the aim or application, a first step in studying the basis of local adaptation is to identify the genes that are driving it.

A potentially powerful method for identifying the genomic regions involved in local adaptation is genotype-environment association (GEA) analysis, which has been widely adopted in recent years. Alleles may vary in frequency across a species' range in response to local environmental conditions that give rise to spatially varying selection pressures (Haldane 1948). For that reason, genetic variants that exhibit strong correlations with putatively selective features of the environment are often interpreted as a signature of local adaptation (Coop et al. 2010). Genotype-environment association (GEA) studies examine such correlations. Allele frequencies for many genetic markers, typically single nucleotide polymorphisms (hereafter SNPs), are estimated in numerous locations across a species' range. Correlations between allele frequency and environmental variables are calculated then contrasted for sites across the genome. It is assumed in GEA studies that current heterogeneity in the environment (whether biotic or abiotic) reflects the history of selection.

Numerous approaches for performing GEA analyses have been proposed. If individuals are sequenced, GEA can be performed by regressing environments on genotypes as a form of genome-wide association study, for example using the *GEMMA* package (Zhou, Carbonetto, and Stephens 2013). However, to estimate SNP effects with reasonable statistical power, many individuals may need to be sequenced. A cost-effective alternative is pooled sequencing (hereafter pooled-seq), where allele frequencies for populations of individuals are estimated rather than individual genotypes (Schlötterer et al. 2014). In this study, we focus on analyses that can be performed on pooled-seq datasets given the wide adoption of that protocol in the GEA literature.

The most straightforward way to perform a GEA analysis is to simply examine the correlation between allele frequencies and environmental variables measured in multiple populations, for example using rank correlations such as Spearman's  $\rho$  or Kendall's  $\tau$ . This simple approach may commonly lead to false positives, however, if there is environmental variation across the focal species' range that is correlated with patterns of gene flow or historical selection (Meirmans 2012; Novembre and Di Rienzo 2009). For example, consider a hypothetical species inhabiting a large latitudinal range. If it had restricted migration and exhibited isolation-by-distance, neutral alleles may be

correlated with any environmental variable that happened to correlate with latitude, as population structure would also correlate with latitude.

Several approaches have been proposed to identify genotype-environment correlations above and beyond what is expected given an underlying pattern of population structure and environmental variation. For example, the commonly used *BayPass* package (Gautier 2015), an extension of *BayEnv* by Coop et al. (2010), estimates correlations between alleles and environmental variables in a two-step process. First, a population covariance matrix ( $\Omega$ ) is estimated from SNP data. Second, correlations between the frequencies of individual SNPs and environmental variables are estimated treating  $\Omega$  in a manner similar to a random effect in a generalized mixed model. In a recent study, Lotterhos (2019) compared several the most commonly used packages for performing GEA on pooled-sequencing datasets; including *BayPass* (Gautier 2015), latent-factor mixed models (LFMMs) as implemented in the LEA package (Frichot et al. 2013; Frichot and François 2015), redundancy analysis (RDA; see Forester et al. 2016, 2018) and a comparatively simple analysis calculating Spearman's  $\rho$  between allele frequency and environment. Of the methods they tested, Lotterhos (2019) found that the GEA approaches that did not correct for population structure (i.e. Spearman's  $\rho$  and RDA) had higher power to detect local adaptation compared to *BayPass* or LFMMs. In their standard application to genome-wide datasets, all of the GEA analysis methods provide a summary statistic for each marker or SNP.

Individual SNPs may provide very noisy estimates of summary statistics, but closely linked SNPs are not independently inherited and may have highly correlated evolutionary histories. As a way to reduce noise, genome scan studies often aggregate data across adjacent markers into analysis windows based on a fixed physical or genetic distance or number of SNPs (Hoban et al. 2016). In the case of  $F_{ST}$ , the standard measure of population differentiation, there are numerous methods for combining estimates across sites (See Bhatia et al. (2013)). In Weir and Cockerham's (1984) method, for example, estimates of  $F_{ST}$  for individual loci are combined into a single value with each marker's contribution weighted by its expected heterozygosity.

In the context of GEA studies, each marker or SNP provides a test of whether a particular genealogy is correlated with environmental variation. In the extreme case of a non-recombining region, all SNPs present would share the same genealogy and thus provide multiple tests of the same hypothesis. The SNPs that are the most informative in this context are those with the highest heterozygosities as they contain the most information about the shape of the underlying genealogy. For recombining portions of the genome, however, linked sites will not have exactly the same genealogy, but genealogies may be highly correlated. Similar to combining estimates of  $F_{ST}$  to decrease statistical noise, combining GEA tests performed on individual markers may increase the power of GEA studies to identify genomic regions that contribute to local adaptation.

In this study, we propose a general method for combining the results of single SNP GEA scores into analysis windows that we call the weighted-Z analysis (WZA). We test the efficacy of WZA using simulations. We generate datasets modelling a pooled-sequencing experiment where estimates of allele frequency are obtained for numerous

populations across a species' range. Using our simulated data, we compare the performance of WZA to Kendall's  $\tau$  as well as *BayPass* (Gautier 2015), as it is a widely used approach that corrects for population structure in GEA studies. Additionally, we compare WZA to another window-based GEA approach that was proposed by Yeaman et al. (2016). We found that the WZA is particularly useful when GEA analysis is performed on small samples and when results for individual SNPs are statistically noisy. We re-analyze previously published lodgepole pine data using the WZA and find several candidate loci that were not identified using the methods of the original study.

## The Weighted-Z Analysis

In this study, we propose the Weighted-Z Analysis (hereafter, the WZA) for combining information across linked sites in the context of GEA studies. The WZA uses the weighted-Z test from the meta-analysis literature that combines  $p$ -values from multiple independent hypothesis tests into a single score (Mosteller and Bush 1954; Liptak 1958; Stouffer et al. 1949). In the weighted-Z test, each of the  $n$  independent tests is given a weight that is proportional to the inverse of its error variance (Whitlock 2005). In the WZA, we use  $\bar{p}\bar{q}$ , a marker's expected heterozygosity, to determine these weights. At a given polymorphic site, we denote the average frequency of the minor allele across populations as  $\bar{p}$  ( $\bar{q}$  corresponds to the frequency of the major allele). Sites with lower values of  $\bar{p}\bar{q}$  will have a greater relative error in estimates of local allele frequency than will sites with higher  $\bar{p}\bar{q}$ , causing greater relative error and bias in estimates of the correlation between allele frequency and an environmental variable. In order to capture this effect approximately we use the same weights as used by Weir and Cockerham (1984) (i.e.,  $\bar{p}\bar{q}$ ) to combine estimates of  $F_{ST}$  across sites.

We combine information from biallelic markers (typically SNPs) present in a focal genomic region into a single weighted-Z score ( $Z_W$ ). The genomic region in question could be a gene or genomic analysis window. We calculate  $Z_{W,k}$  for genomic region  $k$ , which contains  $n$  SNPs as

$$Z_{W,k} = \frac{\sum_{i=1}^n \bar{p}_i \bar{q}_i z_i}{\sqrt{\sum_{i=1}^n (\bar{p}_i \bar{q}_i)^2}}, \quad (1)$$

where  $\bar{p}_i$  is the mean allele frequency across populations and  $z_i$  is the standard normal deviate calculated from the one-sided  $p$ -value for SNP  $i$ . A given  $p$ -value can be converted into a  $z_i$  score using the *qnorm* function in the R programming language, for example.

Under the null hypothesis that there is no correlation between allele frequency and environment and no spatial population structure, the expected distribution of correlation coefficients in a GEA would be normal about 0, with a uniform distribution of  $p$ -values. However, as will often be the case in nature, there may be an underlying correlation between population structure and environmental variation that will cause these genome-wide distributions to deviate from this null expectation. The average effect of population structure on individual SNP scores can be incorporated into an analysis by converting an individual SNP's squared correlation coefficient or parametric  $p$ -value into empirical  $p$ -values based on the genome-wide distribution (following the approach of Hancock et al. [2011]). To calculate empirical  $p$ -values, we rank all values (from smallest to largest in the case of  $p$ -values) and divide the ranks by the total number of tests performed (i.e. the number of SNPs or markers analyzed). Note that in practice, we calculated empirical  $p$ -values after removing SNPs with minor allele frequency less than 0.05 and would recommend that others perform similar filtering. In empirical studies with varying levels of missing data across the genome, it may be preferable to rank the parametric  $p$ -

values rather than the correlation coefficients themselves as there may be varying power to calculate correlations across the genome. With the empirical  $p$ -value procedure, aggregating the empirical  $p$ -values using the WZA will identify genomic regions with a pattern of GEA statistics that deviate from the average genome-wide. A feature of the WZA is that many tests can potentially be used as input as long as individual  $p$ -values provide a measure for the strength of evidence against a null hypothesis.

When we apply the WZA in this study, we used two different statistics as input: empirical  $p$ -values calculated from the genome-wide distribution of parametric  $p$ -values from Kendall's  $\tau$  correlating the local environmental variable and local allele frequency (referred to as  $WZA_{\tau}$ ), and empirical  $p$ -values calculated from the genome-wide distribution of Bayes factors as obtained using the *BayPass* program (referred to as  $WZA_{BP}$ ; see below). Note that Lotterhos (2019) identified Spearman's  $\rho$  as having among the highest power of the GEA analyses that they had tested. We used Kendall's  $\tau$  as it calculates accurate  $p$ -values in the presence of tied datapoints.

## Materials and Methods

### Simulating local adaptation

We performed forward-in-time population genetic simulations of local adaptation to determine how well the WZA was able to identify the genetic basis of local adaptation. GEA studies are often performed on large spatially extended populations that may be comprised of hundreds of thousands of individuals. However, it is computationally infeasible to model selection and linkage in long chromosomal segments (>1Mbp) for such large populations. For that reason, we simulated relatively small populations containing 19,600 diploid individuals in total and scaled population genetic parameters so as to model a large population. We based our choice of population genetic parameters on estimates for conifer species. A representative set of parameters is given in Table S1 and in the Appendix we give a breakdown and justification of the parameters we simulated. All simulations were performed in *SLiM* v3.4 (Messer and Haller 2019).

We simulated meta-populations inhabiting and adapting to heterogeneous environments and modelled the population structure on an idealized conifer species. In conifers, strong isolation-by-distance has been reported and overall mean  $F_{ST} < 0.10$  has been estimated in several species (Mimura and Aitken 2007; Mosca et al. 2014). We thus simulated individuals inhabiting a 2-dimensional stepping-stone population made up of 196 demes (i.e. a  $14 \times 14$  grid). Each deme consisted of  $N_d = 100$  diploid individuals. We assumed a Wright-Fisher model so demes did not fluctuate in size over time. Migration was limited to neighboring demes in the cardinal directions and the reciprocal migration rate between demes ( $m$ ) was set to 0.0375 in each possible direction to achieve an overall  $F_{ST}$  for the metapopulation of around 0.04 (Figure S1). As expected under restricted migration, our simulations exhibited a strong pattern of isolation-by-distance (Figure S1). Additionally, we simulated metapopulations with no spatial structure (i.e., finite island models). In these simulations, we used the formula

$$m = \frac{\frac{1}{F_{ST}} - 1}{4N_d196}$$

(Charlesworth and Charlesworth 2010; pp319) to determine that a migration rate between each pair of demes of  $m = 4.12 \times 10^{-4}$  would give a target  $F_{ST}$  of 0.03.

The simulated organism had a genome containing 1,000 genes uniformly distributed onto 5 chromosomes. We simulated a chromosome structure in *SLiM* by including nucleotides that recombined at  $r = 0.5$  at the hypothetical chromosome boundaries. Each chromosome contained 200 segments of 10,000bp each. We refer to these segments as genes for brevity, although we did not model an explicit exon/intron or codon structure. It has been reported that linkage disequilibrium (LD) decays rapidly in conifers, with LD between pairs of SNPs decaying to background levels within 1,000bp or so in several species (Pavy et al. 2012). In our simulations, recombination within genes was uniform and occurred at a rate of  $r = 10^{-7}$  per base-pair, giving a population-scaled recombination rate ( $4N_d r$ ) of 0.0004. The recombination rate between



the genes was set to 0.005, effectively modelling a stretch of 50,000bp of intergenic sequence. Given these recombination rates, LD decayed rapidly in our simulations with SNPs that were approximately 600bp apart having, on average, half the LD of immediately adjacent SNPs in neutral simulations (Figure S1). Thus, patterns of LD decay in our simulations were broadly similar to the patterns reported for conifers.

We incorporated spatial variation in the environment into our simulations using a discretized map of degree days below 0 (DD0) across British Columbia (BC). We generated the discretized DD0 map by first downloading the map of DD0 for BC from ClimateBC (<http://climatebc.ca/>; Wang et al. 2016; Figure 1A). Using Dog Mountain, BC as the reference point in the South-West corner (Latitude = 48.37, Longitude = -122.97), we extracted data in a rectangular grid with edges 3.6 degrees long in terms of both latitude and longitude, an area of approximately  $266 \times 400 \text{ km}^2$  (Figure 1A). We divided this map into a  $14 \times 14$  grid, calculated the mean DD0 scores in each grid cell, converted them into standard normal deviates (i.e. Z-scores) and rounded up to the nearest third. We used the number of thirds of a Z-score as phenotypic optima in our simulations. We refer to this map of phenotypic optima as the *BC* map (Figure 1B).

We used data from the *BC* map to generate two additional maps of environmental variation. First, we ordered the data from the *BC* map along one axis of the  $14 \times 14$  grid and randomised optima along the non-ordered axis. We refer to this re-ordered map as the *Gradient* map (Figure 1C). Second, we generated a map where selection differed over only a small portion of the environmental range. For some species, fitness optima may differ only beyond certain environmental thresholds, leading to a non-normal distribution of phenotypic optima. To model such a situation, we set the phenotypic optimum of 20 demes in the top-right corner of the meta-population to +3 and set the optimum for all other populations to -1. We chose 20 demes as it represented approximately 10% of the total population. We refer to this map as the *Truncated* map (Figure 1D).

We simulated local adaptation using models of either directional or stabilizing selection. In both cases, there were 12 causal genes distributed evenly across four simulated chromosomes that potentially contributed to local adaptation. With directional selection, mutations affecting fitness could only occur at a single nucleotide position in the center of the 12 potentially selected genes. Directionally selected mutations had a spatially antagonistic effect on fitness. In deme  $d$  with phenotypic optimum  $\theta_d$ , the fitness of a selected allele was calculated as  $1 + s_a \theta_d$  for an individual homozygous for a locally beneficial allele (selected alleles were semi-dominant). The fitness affecting alleles had a mutation rate of  $3 \times 10^{-7}$  in simulations modelling directional selection and a fixed  $s_a = 0.003$  (see *Appendix*).

Under stabilizing selection, the mutations that occurred in the 12 genes had a normal distribution of phenotypic effects, with variance  $\sigma_a^2 = 0.5$ . Phenotype-affecting mutations occurred at a rate of  $10^{-10}$  per base-pair in the 12 genes, and could occur at any of the 10,000 sites within a given gene. An individual's phenotype was calculated as the sum

of the effects of all phenotype-affecting mutations. We calculated an individual's fitness using the standard expression for Gaussian stabilizing selection,

$$W_{z_{i,j}} = \exp \left[ \frac{-(f_{i,j} - \theta_d)^2}{2V_s} \right],$$

where  $f_i$  is the phenotype of the  $i^{th}$  individual in environment  $j$  and  $V_s$  is the variance of the Gaussian fitness function (Walsh and Lynch 2018). We set  $V_s = 196$  so that there was a 40% fitness difference between individuals perfectly adapted to the two extremes of the distribution of phenotypic optima. This was motivated by empirical studies of local adaptation that have demonstrated such fitness differences in numerous species (Hereford 2009; Bontrager et al. 2020); see *Appendix*.

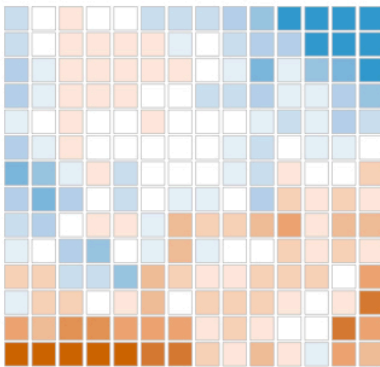
We ran simulations for a total of 200,102 generations. The 19,600 individuals initially inhabited a panmictic population that evolved neutrally. After 100 generations, the panmictic population divided into a  $14 \times 14$  stepping-stone population and evolved strictly neutrally (when modelling directional selection), or with a phenotypic optimum of 0 for all demes (when modelling stabilizing selection). After 180,000 generations, we imposed the various maps of phenotypic optima and simulated for a further 20,000 generations. For selected mutations, we used the "*f*" option for *SLiM*'s mutation stack policy, so only the first mutational change was retained. Using the tree-sequence option in *SLiM* (Haller et al. 2019) we tracked the coalescent history of each individual in the population. At the end of each simulations, neutral mutations were added at a rate of  $10^{-8}$  using *PySLiM* (<https://pyslim.readthedocs.io/en/latest/>). For each combination of map and mode of selection, we performed 20 replicate simulations.

**A**



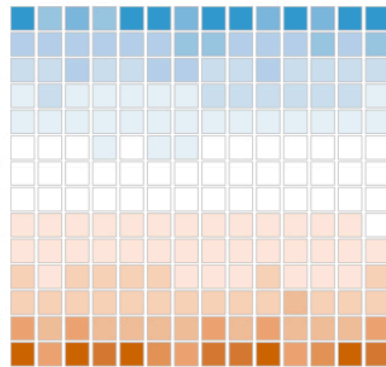
**B**

BC Map



**C**

Gradient Map



**D**

Truncated Map

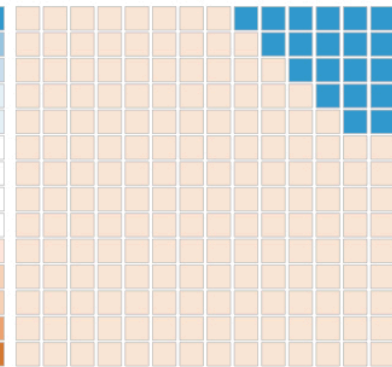


**Figure 1** A) Degree days below zero across British Columbia, the overlain grid in A shows the locations we used to construct phenotypes for our simulated populations. B) A discretized map of DD0 in Southern British Columbia, we refer to the map in B as the *BC map*. C) A 1-dimensional gradient of phenotypic optima, we refer to this as the Gradient map. D) A model of selection acting on a small proportion of the population, we refer to this map as the Truncated map.

## Classifying simulated genes as locally adapted

To evaluate the performance of different GEA methods, we needed to identify which genes contribute to local adaptation and which do not in our simulated data. While there were only 12 genes that were allowed to affect fitness in our simulations, not all of those need be used by the evolving population to result in local adaptation. As described above, our simulations incorporated a stochastic mutation model so from replicate to replicate the genes that contributed to local adaptation varied and, in the case of stabilizing selection, so did the effect size of the alleles in those genes.

For simulations modelling directional selection, we identified locally adapted genes based on the mean fitness of their alleles. For a given gene containing directionally selected alleles, our measure of local adaptation was the covariance between the mean fitness contributed by the selected allele in each population and the environment.

For simulations modelling stabilizing selection, we identified locally adapted genes based on the covariance of the environment and the phenotypic effects of their alleles, summed across all variant sites within each gene. For a given gene, we summed the additive phenotypic effects of all non-neutral variants and took the average for each population. Our measure of local adaptation for each gene was the covariance between that average additive phenotypic effect and environmental variation (we refer to this as  $Cov(Phen, Env)$ ).

For both selection regimes, we defined locally adapted genes as those with a covariance between environment and allelic effect (in fitness or phenotypic terms) greater than 0.005. When assuming directional selection, an average of 6.35, 6.50 and 5.80 genes (out of 12) contained genetic variants that established and contributed to local adaptation for the *BC map*, the Gradient map and the Truncated map, respectively. In our simulations assuming stabilizing selection, individuals' and population mean phenotypes closely matched the phenotypic optima of their local environment (Figure S2). The average numbers of genes contributing to local adaptation in individual replicates in these simulations were 7.15, 6.45 and 5.35 for the *BC map*, the Gradient map and the Truncated map, respectively. However, when analyzing stabilizing selection simulations, we calculated the proportion of the total  $Cov(Phen, env)$  explained by a particular set of genes rather the number of true positives.

## Analysis of simulation data

We performed GEA on our simulated data using either Kendall's  $\tau$ -b (hereafter Kendall's  $\tau$ ), a rank correlation that does not model population structure, or *BayPass*, which corrects for a population covariance matrix (Gautier 2015). For all analyses, except where specified, we analyzed data for a set of 40 randomly selected demes and sampled 50 individuals from each to estimate allele frequencies. We sampled individuals from the same set of demes for all analyses, shown in Figure S3. Each simulation replicate included 1,000 genes, and after excluding alleles with a minor allele frequency less than 0.05 there was an average of 23.3 SNPs per gene. We ran

*BayPass* following the "worked example" in section 5.1.2 of the manual provided with the software.

We used three different methods to summarize the GEA results for each gene in a given simulation replicate: a single SNP-based approach, the WZA and the top-candidate method developed by Yeaman et al. (2016). For all three tests, we used either the  $p$ -values from Kendall's  $\tau$  or *BayPass*.

- For the implementation of the single SNP-based approach, the SNPs with the most extreme test statistic (i.e. smallest  $p$ -value or largest Bayes factor) for each gene were recorded and other SNPs in the gene were subsequently ignored. This was done to prevent multiple outliers that are closely linked from being counted as separate hits. The single-SNP based method is perhaps most similar to how GEA analyses are typically interpreted, as it relies upon the evidence from the most strongly associated SNP to assess significance for a closely linked gene.
- We implemented a simplified version of the top-candidate method proposed by Yeaman et al (2016). The top-candidate method attempts to identify regions of the genome involved in local adaptation under the assumption that such regions may contain multiple sites that exhibit strong correlation with environmental variables. The top-candidate method asks whether there is a significant excess of "outlier" SNPs in a region compared to what one would expect given the genome wide distribution. The number of outliers in a given genomic region is compared to the expected number of outliers based on the genome-wide proportion of SNPs that are outliers, using a binomial test. The  $p$ -value from the binomial test is used as a continuous index.
- For the implementation of the WZA, we converted the  $p$ -values (from Kendall's  $\tau$  or Bayes factors (from *BayPass*), into empirical  $p$ -values. For each of the  $n$  SNPs present in a gene, empirical  $p$ -values were converted into  $z$  scores and used to calculate WZA scores using Equation 1.

We examined effect of variation in recombination on the properties of the WZA by manipulating the tree-sequences that we recorded in *SLiM*. In our simulations, genes were 10,000 bp long, so to model genomic regions of low recombination rate, we extracted the coalescent trees that corresponded to the central 1,000bp or 100bp of each gene. For the 1,000bp and 100bp intervals, we added mutations at 10 $\times$  and 100 $\times$  the standard mutation rate, respectively.

All SNPs present in each 10,000bp gene in our simulations were analyzed together. However, to explore the effect of window size on the performance of the WZA, we calculated WZA scores for variable numbers of SNPs. In these cases, we calculated WZA scores for all adjacent sets of  $g$  SNPs and retained the maximum WZA score for all sets of SNPs in the gene.

Tree sequences were manipulated using the *tskit* package. Mutations were added to trees using the *msprime* (REF), *tskit* and *PySLiM* workflow (version).  $F_{ST}$  and  $r^2$  (an estimator of linkage disequilibrium) were calculated using custom Python scripts that

invoked the *scikit-allel* package (REF).

### Analysis of data from lodgepole pine

We re-analyzed a previously published population genomic dataset for lodgepole pine, *Pinus contorta*, a conifer that is widely distributed across the Northwest of North America. Briefly, Yeaman et al. (2016) collected samples from 254 populations across British Columbia and Alberta, Canada and Northern Washington, USA. The lodgepole pine genome is very large (20Gbp), so Yeaman et al. (2016) used a sequence capture technique based on the *P. contorta* transcriptome. Allele frequencies were estimated for many markers across the captured portion of the genome by sequencing 1-4 individuals per population. Yeaman et al. (2016) performed GEA on each SNP using Spearman's  $\rho$  and used their top-candidate method (see above) to aggregate data across sites within genes. We downloaded the data for individual SNPs from the Dryad repository associated with Yeaman et al. (2016) (<https://doi.org/10.5061/dryad.0t407>). We converted Spearman's  $\rho$   $p$ -values into empirical  $p$ -values and performed WZA on the same genes analyzed by Yeaman et al (2016). We also repeated the top-candidate method, classifying SNPs with empirical  $p$ -values  $< 0.01$  as outliers. However, as above, we use the  $p$ -value from the top-candidate method as a continuous index.

### Data and Code Availability

The simulation configuration files and code to perform the analysis of simulated data and generate the associated plots are available at [github/TBooker/GEA/WZA](https://github.com/TBooker/GEA/WZA). Analyses were performed using a combination of R and Python. All plots were made using *ggplot2* (REF). Tree-sequence files for the simulated populations are available at Dryad and all processed GEA files are available on (SomeCoolLocation).



## Results

### The statistical properties of the WZA

To assess the statistical properties of the WZA, we first performed GEA analyses on populations that were evolving neutrally. Figure 2A shows the distribution of  $WZA_{\tau}$  scores for stepping-stone populations simulated under the *BC Map*. The null expectation for WZA scores is the standard normal distribution (mean of 0 and standard deviation of 1), but we found that the distribution of  $WZA_{\tau}$  scores deviated slightly from this even under neutrality, where the mean and standard deviation of  $WZA_{\tau}$  scores from individual simulation replicates were approximately 0.089 and 1.38, respectively. Additionally, the inset histogram in Figure 2A shows that distribution of  $WZA_{\tau}$  scores had a thicker right-hand tail than expected under the normal distribution.

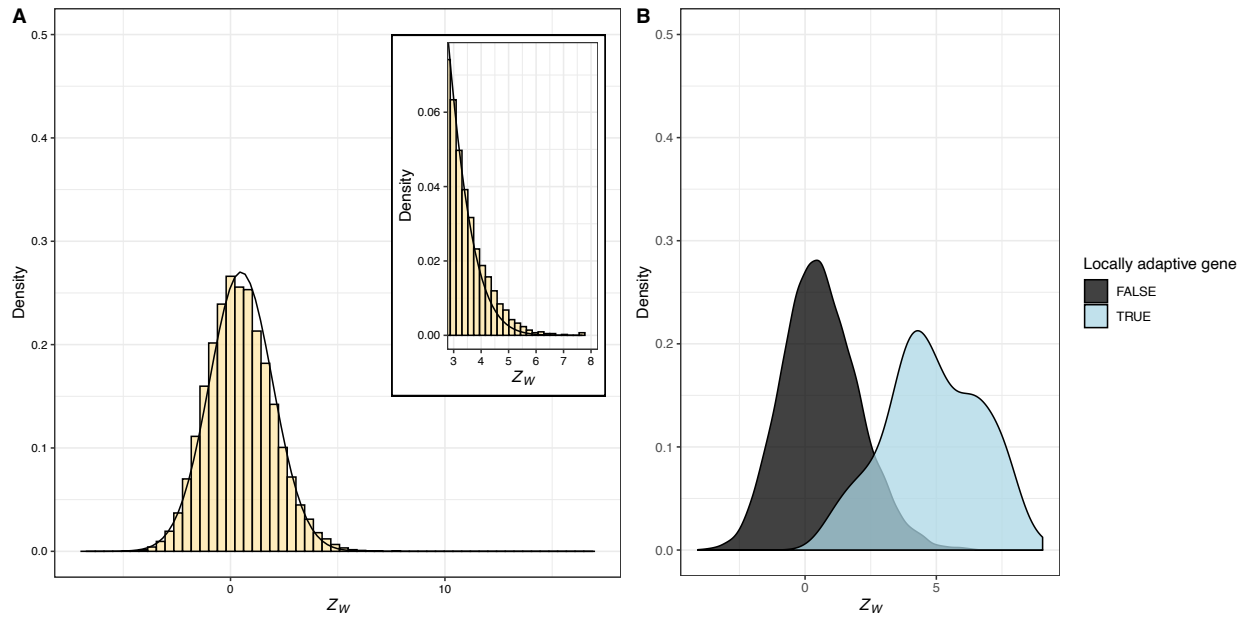


**Figure 2.** The distribution of WZA scores under neutrality and a model of local adaptation. A) A histogram of  $WZA_{\tau}$  scores under strict neutrality across a set of 20 replicate simulations, inset is a close-up view of the upper tail of the distribution of  $Z_W$  scores. B) A density plot showing the separation of  $WZA_{\tau}$  scores for genes that are locally adaptive versus evolving neutrally across the genome of 20 simulation replicates. GEA was performed on 40 demes sampled from the *BC Map*.

The deviation from the standard normal distribution is driven by non-independence of SNPs within the analysis windows we used to calculate WZA scores. To demonstrate this, we re-calculated WZA scores, but permuted the locations of SNPs across the genome, effectively erasing the signal of linkage within genes. The distribution of  $WZA_{\tau}$  scores in this permuted dataset closely matched the null expectation and did not have a thick right-hand tail (Figure S4; shuffled); each of 20 simulation replicates had mean a

WZA $\tau$  indistinguishable from 0 with a standard deviation very close to 1. It is worth noting that we modelled populations that did not change in size over time. Non-equilibrium population dynamics such as population expansion may influence the distribution of WZA scores.

When evolution includes selection, WZA can often clearly distinguish regions of the genome containing loci that contribute to local adaptation from those that do not. Figure 2B shows clear separation of WZA $\tau$  scores for genes that contribute to local adaptation from those that are evolving neutrally (similar results were found for both the *Gradient* and *Truncated* maps; Figure S5). The distributions of WZA $\tau$  scores for locally adapted genes when modelling stabilizing selection was broader than when modelling directional selection (Figure S5), consistent with differences in the distributions of effect size for the genes involved in local adaptation under the two selection models (Figure S6). The separation of the distributions of WZA $\tau$  scores for locally adaptive genes versus neutrally evolving genes indicates that it may be a powerful method for identifying the genetic basis of local adaptation.

### Comparison of the WZA with other GEA approaches

We compared WZA to two other methods for identifying genomic regions that contribute to local adaptation from GEA data (Figure 3). To assess the performance of the different methods, we examined the top 1, 2, 3,... 50 genes in terms of WZA $\tau$  scores,  $-\log_{10}(p\text{-values})$  from the top-candidate method, or the single SNP Kendall's  $\tau$  approach and calculated the proportion of all true positives that were identified in each case. In our simulations, there were 1,000 genes in total with around 6 locally adapted genes in each replicate (see Methods). For visualization purposes, we include Figure S7, which shows the  $-\log_{10}(p\text{-values})$  from Kendall's  $\tau$  represented as a Manhattan plot for individual simulation replicates, WZA $\tau$  and top-candidate scores calculated from those data and the proportion of true positives detected using the three different analysis methods.



Figure 3 compares the performance of the GEA methods across the three different maps of environmental variation that we simulated. Empirical GEA studies may vary substantially in terms of how many populations or demes are sampled. For each of the three maps we simulated, we analyzed samples of 10, 20 or 40 demes where allele frequencies were estimated from 50 individuals sampled in each location; Figure SF shows the specific demes we sampled in each case. Figure 3 shows that  $WZA_{\tau}$  substantially outperformed both the top-candidate and single SNP-based Kendall's  $\tau$  analyses in many cases. When analyzing simulations that used the *BC* map or the *Truncated* map,  $WZA_{\tau}$  always outperformed the top-candidate and SNP-based methods, but particularly so when fewer demes were sampled (Figure 3). When simulations assumed the *Gradient* map,  $WZA_{\tau}$  outperformed the other GEA methods when the sample was restricted to 10 demes, but with larger samples, the tests were more similar (Figure 3). This suggests that  $WZA_{\tau}$  is a powerful method for identifying regions of the genome that contribute to local adaptation in empirical analyses, but particularly so when they are performed on small samples.

An additional source of variation in GEA studies comes from the number of individuals sampled in each location. We also examined the effect that reduced sampling of individuals within each deme had on the performance of the methods. Figure S8 shows that the WZA outperforms the top-candidate and SNP-based methods when a small number of individuals is used to estimate allele frequencies. Note that this is not strictly a test of how well pooled-seq will perform with small sample sizes, however. With small numbers of individuals in sequencing pools, differential amounts of DNA from each individual may add to error in allele frequency estimation (Schlötterer et al. 2014).

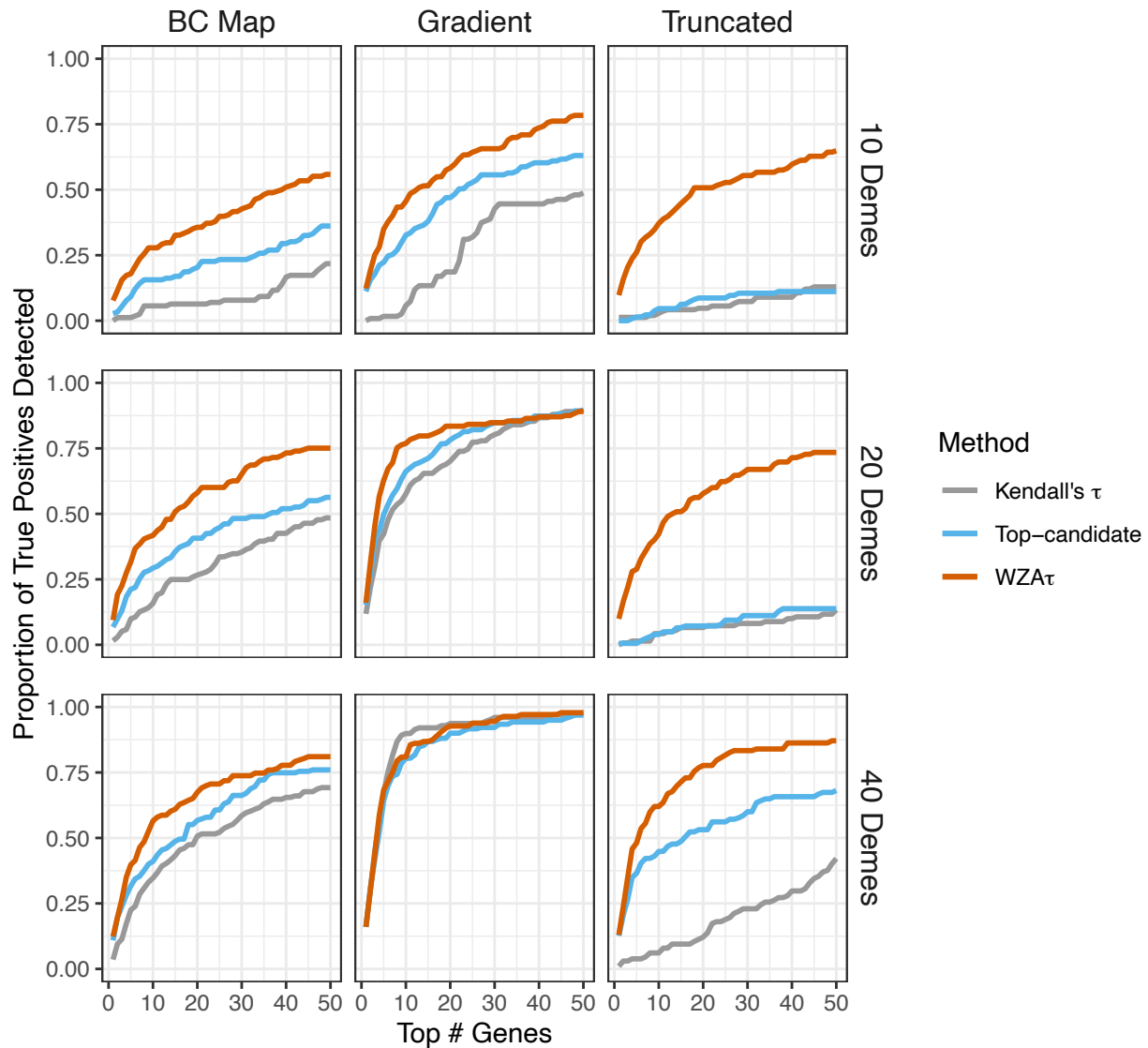


**Figure 3** A comparison of three methods to identify outliers in GEA analysis conducted on simulations modelling local adaptation via directional selection. Plots show the proportion of true positives identified by examining the genes with the top ranked scores across the genome for the three GEA methods. The rows of the plot show results obtained from samples of 10, 20 or 40 demes as indicated by the labels on the right-hand side. Lines represent the means of 20 simulation replicates.

### Effects of population structure correction

In each of the maps of environmental variation that we simulated, there was a strong correlation between environmental variables and gene flow. Environmental variation in each map was autocorrelated along a major axis: the diagonal axis from the bottom-left corner to the top right-corner in the case of the *BC* map (Figure 1B), the vertical axis in the case of the *Gradient* map (Figure 1C), and the top-right corner versus the rest of the

landscape in the case of the *Truncated* map (Figure 1D). There was also a strong pattern of isolation-by-distance in our simulated populations (Figure S1). These two factors may make it difficult to identify genes involved in local adaptation in GEA studies (Meirmans 2012).

We compared the performance of the WZA to a widely adopted method for performing GEA that corrects for the confounding effects of population structure, *BayPass* (Gautier 2015). In all cases, WZA performed as well, or better than, *BayPass* (Figure 4). WZA performed much better than *BayPass* when selection was directional, but WZA was also significantly more likely to identify the genes underlying local adaptation with stabilizing selection.

Notably, even the single SNP analyses based on Kendall's  $\tau$  in most cases outperformed *BayPass*, even though the Kendall's  $\tau$  analysis did not adjust for spatial population structure. (The exception was the case with stabilizing selection on the *Truncated* map.) The discriminatory power of GEAs does not seem to be improved consistently by careful accounting of the underlying pattern of genetic structure.

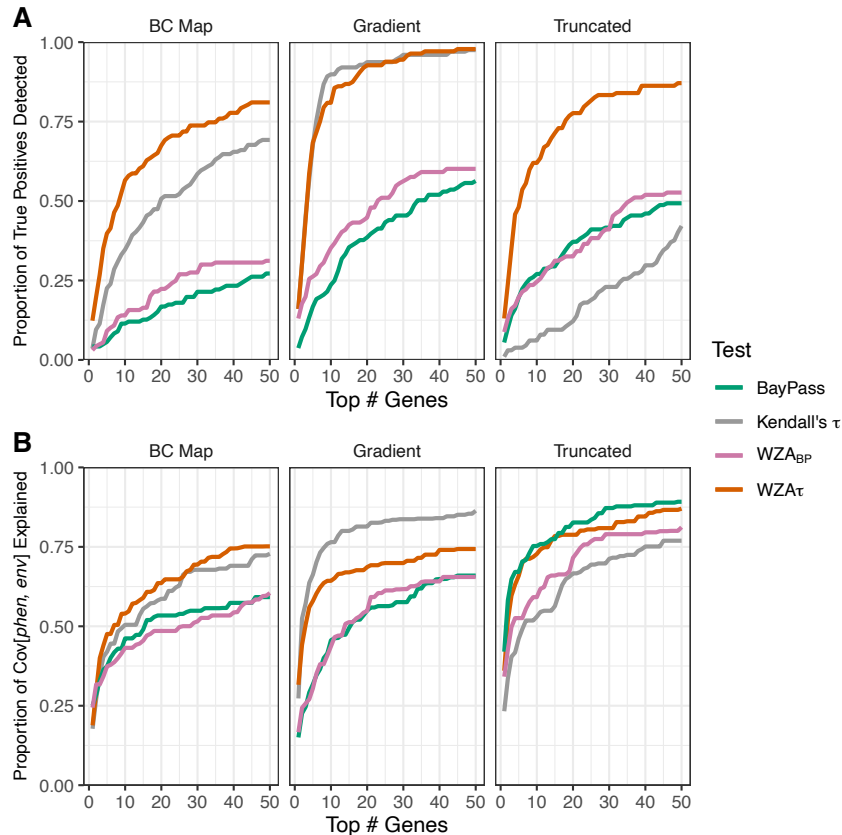


**Figure 4** The performance of population structure correction. A) Results for simulations modelling directional selection and b) results for simulations modelling stabilizing selection. Lines represent the mean of 20 simulation replicates.

## The performance of WZA when environmental variables are weakly correlated with selection pressure

In the previous section, we conducted GEA assuming perfect knowledge of the phenotypic optima in each sampled deme. However, in empirical GEA analyses researchers will be probably always be limited to studying environmental variables that are imperfect proxies for historical selection patterns. Additionally, environmental variables are often obtained via interpolation and/or may be measured with error. These factors mean that the “E” in GEA will probably always be imperfectly correlated with historical selection. The strength of that correlation will, of course, determine power in GEA studies. Using the simulations modelling local adaptation on the *BC* map via stabilizing selection, we compared the performance of WZA against the single-SNP GEA methods when the measured environment is imperfectly correlated with the phenotypic optima.

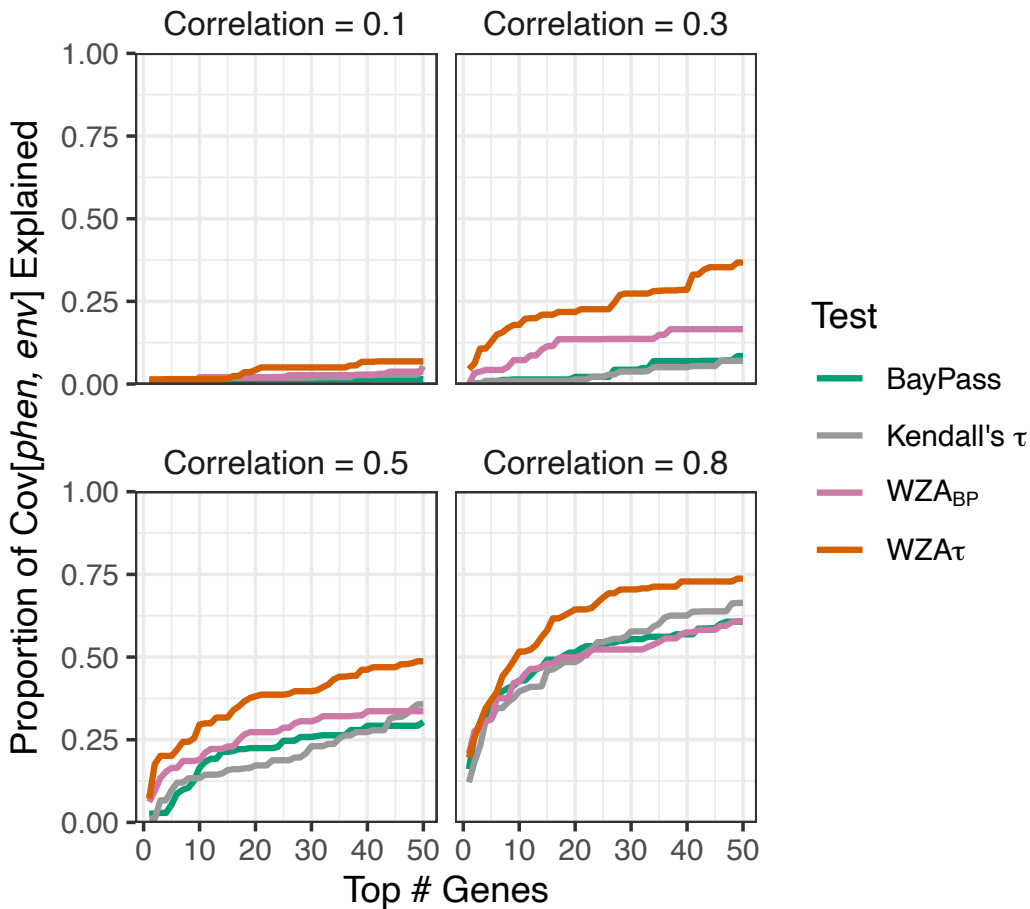


**Figure 5** The proportion of true positives recovered when the measured environment is imperfectly correlated with phenotypic optima. The correlation between environment and selection pressure is shown above each panel. Results are shown assuming the *BC Map* and the model of stabilising selection. Line indicate the means from 20 simulation replicates, and each is based on samples of 50 individuals from each of 40 demes.

We found that the WZA outperformed single SNP approaches (Kendall's  $\tau$  or BayPass) when the measured environment was not perfectly correlated with phenotypic optima. We analyzed a sample of 40 demes from the population with 50 individuals taken in each location (Figure S2) but added random noise to the phenotypic optima from these locations to simulate environmental variables that were variably correlated with selection pressures and with which to conduct GEA. As might be expected, when the correlation between the measured environment and phenotypic optima was very weak (i.e., a correlation of 0.1), very few true positives were present in the top 50 genes under any of the methods we used, and those genes present only accounted for a small proportion of the covariance between phenotype and environment (Figure 5). With a correlation of 0.3 between the measured environment and true selection, WZA $\tau$  outperformed WZA<sub>BP</sub> and the single-SNP approaches (Figure 5). With a correlation of 0.5 or 0.8 between the measured environment and phenotypic optima WZA $\tau$  outperformed all other methods, with only relatively small differences in performance between WZA<sub>BP</sub> and the single-SNP approaches. Overall, this result suggests that WZA $\tau$  outperforms the single-SNP approaches when the measurement of the environment is a poor proxy for historical selection.

### *The width of analysis windows and recombination rate variation*

Random drift may cause genealogies in some regions of the genome to correlate with environmental variables more than others. Many of the SNPs present in an analysis window that consisted of genealogies that were highly correlated with the environment may be highly significant in a GEA analysis, leading to a large WZA score. This effect would lead to a larger variance in WZA scores for analysis windows that were present in regions of low recombination. To demonstrate this, we down-sampled the tree-sequences we recorded for our simulated populations to model analysis windows present in low recombination regions and performed the WZA on the resulting data. As expected, we found that the variance of the distribution of WZA scores was greater when there was a lower recombination rate (Figure S9). This is the same effect we described in a previous paper focusing on  $F_{ST}$  (Booker et al. 2020).

### *Application of the WZA to data from lodgepole pine*

We re-analyzed a previously published (Yeaman et al. 2016) lodgepole pine (*Pinus contorta*) dataset comparing the WZA to the top-candidate method, which had been

developed for the original study. Overall, the WZA and top candidate statistic were broadly correlated and identified many of the same genes as the most strongly associated loci, but also differed in important ways. Across the lodgepole pine genome, there was a mean WZA score of 0.013 with a standard deviation  $\sigma = 1.67$ , and a fat right-hand tail (Figure S11). Figure 6A shows the relationship between WZA scores and the  $-\log_{10}(p\text{-value})$  from the top-candidate method, which were positively correlated (Kendall's  $\tau = 0.245$ ,  $p\text{-value} < 10^{-16}$ ). When many of the SNPs in a gene had strongly associated statistics, both methods would tend to yield high scores (Figure 6D-E). When there were many SNPs with marginally significant empirical  $p$ -values (*i.e.*  $0.05 < p < 0.10$ ) at relatively high frequencies, the WZA method would tend to yield a high score but the top candidate method would not (Figure 6B). By contrast, if the most strongly associated SNPs tended to have low allele frequencies, the top candidate method would tend to yield a high score but the WZA would not (Figure 6C). There were several genes that had WZA scores greater than 10 (approximately  $6\sigma$ ), but very modest top-candidate scores (Figure 6A). Figure 6B shows that for one such region, there were several SNPs with high mean allele frequency that have small  $p$ -values. This particular region had a high score from the top-candidate method. Conversely, Figure 6C shows a region that only had a  $Z_W \approx 5$ , but an extreme score from the top-candidate method. In this case, there were numerous SNPs that passed the top-candidate outlier threshold, but they were mostly at low allele frequency. Figures 6C-D show the relationship between allele frequency and the empirical  $p$ -value for SNPs present in two genes that had extreme scores from both the top-candidate method and the WZA.

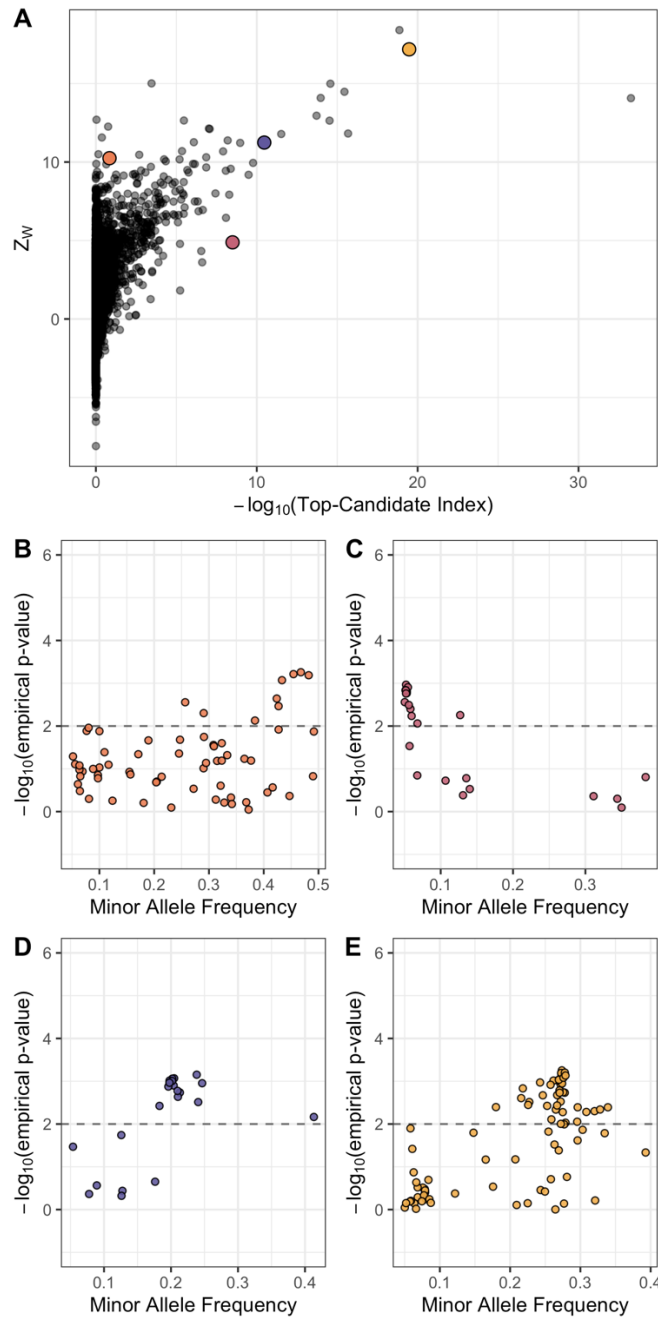


**Figure 6** The WZA applied to GEA results on Lodgepole Pine for degree days below 0 (DD0). A)  $Z_w$  scores compared to scores from the top-candidate method for each of the genes analyzed by Yeaman et al. (2016). Panels B-E show the results for  $-\log_{10}(\text{p-values})$  for Spearman's  $\rho$  applied to individual SNPs against minor allele frequency (MAF) for the colored points in A. The dashed horizontal line in B-D indicates the significance threshold used for the top-candidate method (i.e. 99<sup>th</sup> percentile of GEA  $-\log_{10}(\text{p-values})$  genome-wide).

## Discussion

In this study, we have shown that combining information across linked sites in GEA analyses is a potentially powerful way to identify genomic loci involved in local adaptation. The method we propose, the WZA, was usually more powerful than looking at individual sites in isolation, particularly when working with small samples or when the environmental variation being analyzed is only weakly correlated with selection (Figures 3 and 5). The WZA outperformed the other window-based method we examined, the top-candidate method (Figure 3). In a hypothetical world where one had perfect knowledge of allele frequency variation across a species' range for all sites across the genome, a single marker approach would likely be the best way to perform a GEA analysis, as one would be able to determine the true correlation between genetic and environmental variation for each site in the genome. Indeed, we found that when we had perfect knowledge of allele frequencies in all locations, the SNP-based GEA always outperformed or matched the WZA and top-candidate methods (Figure S13). However, such a situation is unrealistic, and empirical GEA studies will likely always be limited to finite samples from populations of interest. Thus, leveraging the correlated information present among closely linked sites in GEA studies may provide a powerful method for identifying the genetic basis of local adaptation.

Theoretical studies of local adaptation suggest that we should expect regions of the genome subject to spatially varying selection pressures to exhibit elevated linkage disequilibrium (LD) relative to the genomic background for a number of reasons. Under local adaptation, alleles are subject to spatial fluctuation in the direction of selection. As a locally adaptive allele spreads in the locations where it is beneficial, it may cause some linked neutral variants to hitchhike along with it (Sakamoto and Innan 2019). LD can be increased further as non-beneficial genetic variants introduced to local populations via gene flow are removed by selection. This process can be thought of as a local barrier to gene flow acting in proportion to the linkage with a selected site (Barton and Bengtsson 1986). Beyond this hitchhiking signature, there is a selective advantage for alleles that are involved in local adaptation to cluster together, particularly in regions of low recombination (Rieseberg 2001; Noor et al. 2001; Kirkpatrick and Barton 2006; Yeaman 2013). For example, in sunflowers and *Littorina* marine snails, there is evidence that regions of suppressed recombination cause alleles involved in local adaptation to be inherited together (Morales et al. 2019; Todesco et al. 2020). The processes we have outlined are not mutually exclusive, but overall, genomic regions containing strongly selected alleles that contribute to local adaptation may have elevated LD and potentially exhibit GEA signals at multiple linked sites. Window-based GEA scans can potentially take advantage of the LD that is induced by local adaptation, aiding in the discovery of locally adaptive genetic variation.

The two window-based GEA methods we compared in this study, the WZA and the top-candidate method of Yeaman et al. (2016), were fairly similar in power in some cases, but WZA was often better (Figure 3). Moreover, there are philosophical reasons as to why WZA should be preferred over the top-candidate method. Firstly, the top-candidate method requires the use of an arbitrary significance threshold. This is undesirable,



however, because genuine genotype-environment correlations may be very weak and GEA may simply be an underpowered approach to identify alleles that contribute to local adaptation. If there were no detectable signal of local adaptation, ascribing significance to a fraction of the genome may lead to false positives. Secondly, the top-candidate method gives equal weight to all SNPs that have exceeded the significance threshold. For example, with a threshold of  $\alpha = 0.01$ , genomic regions with only a single outlier are treated in the same way whether that outlier has a  $p$ -value of 0.009 or  $10^{-10}$ . It is desirable to retain information about particularly strong outliers. It should be kept in mind, however, that the WZA (and the top-candidate method for that matter) does not explicitly test for local adaptation and only provides an indication of whether a particular genomic region has a pattern that deviates from the genome-wide average. Indeed, numerous processes other than local adaptation may cause excessive correlation between environmental variables and allele frequencies in particular genomic regions. For example, population expansions can cause allelic surfing, where regions of the genome “surf” to high frequency at leading edge of an expanding population. Allelic surfing can leave heterogeneous patterns of variation across a species range leaving signals across the genome that may resemble local adaptation (Novembre and Di Rienzo 2009; Klopstein, Currat, and Excoffier 2006).

When performing a genome-scan using a windowed approach a question that inevitably arises is, how to choose the width of analysis windows? If analysis windows were too narrow, there may be little benefit in using a windowed approach over a single-SNP approach. In all the results presented above, 10,000bp analysis windows were used for the WZA. We found that the performance of the WZA when analysis windows that were narrower than 10,000bp was intermediate between the 10,000bp case and the single-SNP approach (Figure S12). Of course, if analysis windows were too wide, the signal of local adaptation may be diluted and the WZA would have little power. It seems like the ideal width for analysis windows would be informed by the the pattern of recombination rate variation, LD decay and SNP density across a species genome. In practice, it may be useful to perform the WZA on groups of SNPs, such as genes as in the Yeaman et al (2016) study. Future study is required to determine the optimal size for analysis windows.

A striking result from our comparison of the various GEA methods we tested in this study was the low power of *BayPass* compared to Kendall’s  $\tau$  (Figure 4). As mentioned in the Introduction, Lotterhos (2019) obtained a similar result in a previous study, though they had used Spearman’s  $\rho$  rather than Kendall’s  $\tau$ . This presumably occurs because genome-wide population genetic structure is oriented along a similar spatial axis as adaptation, and the correction in *BayPass* therefore causes a reduction in the signal of association at genes involved in adaptation. In such cases, the use of simple rank correlations such as Spearman’s  $\rho$  or Kendall’s  $\tau$ , which assume that all demes are independent, may often yield a skewed distribution of  $p$ -values. Such a distribution would lead to a large number of false positives if a standard significance threshold is used (Meirmans 2012). Here, we avoid standard significance testing, and instead make use of an attractive quality of the distribution of  $p$ -values: SNPs in regions of the genome that contribute to adaptation tend to have extreme  $p$ -values, relative to the genome-wide distribution. By converting them to empirical  $p$ -values, we retain the

information contained in the rank-order of  $p$ -values, but reduce the inflation of their magnitude, which increases the power of the test (Figure S12). While the empirical  $p$ -value approach may partially and indirectly correct for false positives due to population structure genome-wide, it loses information contained in the raw  $p$ -value that represents the deviation of the data from the null model for our summary statistic of interest. A GEA approach that produced parametric  $p$ -values that was adequately controlled for population structure may provide a more powerful input statistic to the WZA.

Perhaps more striking was how underpowered these GEA methods were at identifying the genes involved in local adaptation. In our simulations, around 6 locally adaptive genes established in each replicate in each of the cases we tested. When analyzing our simulations, we examined the true positives present in the top 1, 2, 3, ..., 50 genes, but in most cases, the proportion of all true positives identified did not reach 1.0 (Figures 3-5), indicating high false discovery rates. Each simulation replicate included 1,000 genes, so the top 50 represents the 95<sup>th</sup> percentile of the genome-wide distribution. Examining the upper percentiles of the empirical distribution of GEA scores is an approach taken in empirical analyses (e.g. Shi et al. 2021; Leigh et al. 2021), though it would perhaps be preferable to have a threshold that was applied to an appropriate null distribution. One drawback of the WZA is that since the distribution of WZA scores was non-normal even under neutrality (Figure 2), we cannot compute a parametric  $p$ -value for each analysis window tested. *BayPass*, on the other hand, returns a Bayes factor for each analyzed SNP, the log-transformed ratio of the likelihoods under the alternate and null hypotheses. A general rule of thumb for the interpretation of Bayes factors is that BFs > 20 are considered strong evidence against the null hypothesis (i.e., Jeffrey's rule). Overall, applying a stringent Bayes factor threshold to *BayPass* may result in a test with low false positive rates, the WZA may provide a more sensitive test at the cost of specificity.

Ultimately, performing GEA analyses using analysis windows is an attempt to leverage information from closely linked sites. With the advent of methods for reconstructing ancestral recombination graphs from population genomic data (Hejase et al. 2020), perhaps a GEA method could be developed that explicitly analyzes inferred genealogies rather than individual markers in a manner similar to regression of phenotypes on genealogies proposed by Ralph et al. (2020). Such a method would require large numbers of individuals with phased genome sequences, which may now be feasible given recent technological advances (Meier et al. 2021).

In conclusion, theoretical models of local adaptation suggest that we should expect elevated LD in genomic regions subject to spatially varying selection pressures. For that reasons, GEA analyses may gain power by making use of information encoded in patterns of tightly linked genetic variation. The method we proposed in this study, the WZA, outperforms single-SNP approaches in a range of settings so provides researchers with a powerful tool to characterize the genetic basis of local adaptation in population and landscape genomic studies.

## Acknowledgements

Thanks to Pooja Singh for many helpful discussions, to Tongli Wang for help with BC climate data and to Simon Kapitza for help with wrangling raster files. Thanks to Finlay Booker for moral support throughout the course of this project. TRB is supported by funding from Genome Canada, Genome Alberta and NSERC Discovery Grants awarded to MCW and SY. SY is supported by an AIHS research chair and NSERC Discovery Grant. MCW is supported by an NSERC Discovery Grant. Computational Support was provided by Compute Canada. This study is part of the CoAdapTree project which is funded by Genome Canada (241REF), Genome BC and 16 other sponsors (<http://coadapttree.forestry.ubc.ca/sponsors/>).

## Bibliography

- Aitken, Sally N, and Michael C Whitlock. 2013. "Assisted Gene Flow to Facilitate Local Adaptation to Climate Change." *Annu. Rev. Ecol. Evol. Syst.* 44 (1): 367–88.
- Barton, Nick, and Bengt Olle Bengtsson. 1986. "The barrier to genetic exchange between hybridising populations." *Heredity* 57 (3): 357–76.  
<https://doi.org/10.1038/hdy.1986.135>.
- Bhatia, Gaurav, Nick Patterson, Sriram Sankararaman, and Alkes L. Price. 2013. "Estimating and interpreting FST: The impact of rare variants." *Genome Research* 23 (9): 1514–21. <https://doi.org/10.1101/gr.154831.113>.
- Bontrager, M., C. D. Muir, C. Mahony, D. E. Gamble, R. M. Germain, A. L. Hargreaves, E. J. Kleyhans, K. A. Thompson, and A. L. Angert. 2020. "Climate warming weakens local adaptation." *bioRxiv*. <https://doi.org/10.1101/2020.11.01.364349>.
- Booker, Tom R., Sam Yeaman, and Michael C. Whitlock. 2020. "Variation in recombination rate affects detection of outliers in genome scans under neutrality." *Molecular Ecology* 29 (22): 4274–9. <https://doi.org/10.1111/mec.15501>.
- Charlesworth, B, and D Charlesworth. 2010. *Elements of Evolutionary Genetics*. Book. Greenwood Village, Colorado: Roberts & Company.
- Coop, Graham, David Witonsky, Anna Di Rienzo, and Jonathan K. Pritchard. 2010. "Using environmental correlations to identify loci underlying local adaptation." *Genetics* 185 (4): 1411–23. <https://doi.org/10.1534/genetics.110.114819>.
- Forester, Brenna R., Matthew R. Jones, Stéphane Joost, Erin L. Landguth, and Jesse R. Lasky. 2016. "Detecting spatial genetic signatures of local adaptation in heterogeneous landscapes." *Molecular Ecology* 25 (1): 104–20.  
<https://doi.org/10.1111/mec.13476>.
- Forester, Brenna R., Jesse R. Lasky, Helene H. Wagner, and Dean L. Urban. 2018. "Comparing methods for detecting multilocus adaptation with multivariate genotype-environment associations." *Molecular Ecology* 27 (9): 2215–33.  
<https://doi.org/10.1111/mec.14584>.
- Frichot, Eric, and Olivier François. 2015. "LEA: An R package for landscape and ecological association studies." Edited by Brian O'Meara. *Methods in Ecology and Evolution* 6 (8): 925–29. <https://doi.org/10.1111/2041-210X.12382>.
- Frichot, Eric, Sean D. Schoville, Guillaume Bouchard, and Olivier François. 2013. "Testing for Associations between Loci and Environmental Gradients Using Latent Factor Mixed Models." *Molecular Biology and Evolution* 30 (7): 1687–99.  
<https://doi.org/10.1093/molbev/mst063>.

781 Gautier, Mathieu. 2015. "Genome-wide scan for adaptive divergence and association  
782 with population-specific covariates." *Genetics* 201 (4): 1555–79.  
783 <https://doi.org/10.1534/genetics.115.181453>.

784 Haldane, J. B. S. 1948. "The theory of a cline." *Journal of Genetics* 48 (3): 277–84.  
785 <https://doi.org/10.1007/BF02986626>.

786 Haller, Benjamin C, Jared Galloway, Jerome Kelleher, Philipp W Messer, and Peter L  
787 Ralph. 2019. "Tree-sequence recording in SLiM opens new horizons for forward-time  
788 simulation of whole genomes." *Mol. Ecol. Resour.* 19 (2): 552–66.

789 Hancock, Angela M., Benjamin Brachi, Nathalie Faure, Matthew W. Horton, Lucien B.  
790 Jarymowycz, F. Gianluca Sperone, Chris Toomajian, Fabrice Roux, and Joy Bergelson.  
791 2011. "Adaptation to climate across the *Arabidopsis thaliana* genome." *Science* 334  
792 (6052): 83–86. <https://doi.org/10.1126/science.1209244>.

793 Hejase, Hussein A., Noah Dukler, and Adam Siepel. 2020. "From Summary Statistics to  
794 Gene Trees: Methods for Inferring Positive Selection." Elsevier Ltd.  
795 <https://doi.org/10.1016/j.tig.2019.12.008>.

796 Hereford, Joe. 2009. "A quantitative survey of local adaptation and fitness trade-offs."  
797 The University of Chicago Press. <https://doi.org/10.1086/597611>.

798 Hoban, Sean, Joanna L. Kelley, Katie E. Lotterhos, Michael F. Antolin, Gideon  
799 Bradburd, David B. Lowry, Mary L. Poss, Laura K. Reed, Andrew Storfer, and Michael  
800 C. Whitlock. 2016. "Finding the genomic basis of local adaptation: Pitfalls, practical  
801 solutions, and future directions." *American Naturalist* 188 (4): 379–97.  
802 <https://doi.org/10.1086/688018>.

803 Kirkpatrick, Mark, and Nick Barton. 2006. "Chromosome inversions, local adaptation  
804 and speciation." *Genetics* 173 (1): 419–34. <https://doi.org/10.1534/genetics.105.047985>.

805 Klopstein, Seraina, Mathias Currat, and Laurent Excoffier. 2006. "The fate of mutations  
806 surfing on the wave of a range expansion." *Molecular Biology and Evolution*.  
807 <https://doi.org/10.1093/molbev/msj057>.

808 Legendre, P., and L. Legendre. 2012. *Numerical Ecology, Volume 24*. 3rd Englis.  
809 Elsevier. [https://www.elsevier.com/books/numerical-ecology/legendre/978-0-444-53868-](https://www.elsevier.com/books/numerical-ecology/legendre/978-0-444-53868-0)  
810 [0](https://www.elsevier.com/books/numerical-ecology/legendre/978-0-444-53868-0).

811 Lotterhos, Katie E. 2019. "The Effect of Neutral Recombination Variation on Genome  
812 Scans for Selection." *G3* 9 (6): 1851–67.

813 Meirmans, Patrick G. 2012. "The trouble with isolation by distance." *Molecular Ecology*  
814 21 (12): 2839–46. <https://doi.org/10.1111/j.1365-294X.2012.05578.x>.

815 Mimura, M., and S. N. Aitken. 2007. "Adaptive gradients and isolation-by-distance with  
816 postglacial migration in *Picea sitchensis*." *Heredity* 99 (2): 224–32.  
817 <https://doi.org/10.1038/sj.hdy.6800987>.

818 Morales, Hernán E., Rui Faria, Kerstin Johannesson, Tomas Larsson, Marina Panova,  
819 Anja M. Westram, and Roger K. Butlin. 2019. "Genomic architecture of parallel  
820 ecological divergence: Beyond a single environmental contrast." *Science Advances* 5  
821 (12): eaav9963. <https://doi.org/10.1126/sciadv.aav9963>.

822 Mosca, Elena, Santiago C. González-Martínez, and David B. Neale. 2014.  
823 "Environmental versus geographical determinants of genetic structure in two subalpine  
824 conifers." *New Phytologist* 201 (1): 180–92. <https://doi.org/10.1111/nph.12476>.

825 Noor, M. A. F., K. L. Gratos, L. A. Bertucci, and J. Reiland. 2001. "Chromosomal  
826 inversions and the reproductive isolation of species." *Proceedings of the National  
827 Academy of Sciences of the United States of America* 98 (21): 12084–8.  
828 <https://doi.org/10.1073/pnas.221274498>.

829 Novembre, John, and Anna Di Rienzo. 2009. "Spatial patterns of variation due to natural  
830 selection in humans." *Nat Rev Genet.* <https://doi.org/10.1038/nrg2632>.

831 Pavy, N., M. C. Namroud, F. Gagnon, N. Isabel, and J. Bousquet. 2012. "The  
832 heterogeneous levels of linkage disequilibrium in white spruce genes and comparative  
833 analysis with other conifers." *Heredity* 108 (3): 273–84.  
834 <https://doi.org/10.1038/hdy.2011.72>.

835 Ralph, Peter, Kevin Thornton, and Jerome Kelleher. 2020. "Efficiently summarizing  
836 relationships in large samples: A general duality between statistics of genealogies and  
837 genomes." *Genetics* 215 (3): 779–97. <https://doi.org/10.1534/genetics.120.303253>.

838 Rieseberg, Loren H. 2001. "Chromosomal rearrangements and speciation." Elsevier.  
839 [https://doi.org/10.1016/S0169-5347\(01\)02187-5](https://doi.org/10.1016/S0169-5347(01)02187-5).

840 Sakamoto, Takahiro, and Hideki Innan. 2019. "The evolutionary dynamics of a genetic  
841 barrier to gene flow: From the establishment to the emergence of a peak of divergence."  
842 *Genetics* 212 (4): 1383–98. <https://doi.org/10.1534/genetics.119.302311>.

843 Schlötterer, Christian, Raymond Tobler, Robert Kofler, and Viola Nolte. 2014.  
844 "Sequencing pools of individuals-mining genome-wide polymorphism data without big  
845 funding." Nature Publishing Group. <https://doi.org/10.1038/nrg3803>.

846 Stapley, Jessica, Philine G. D. Feulner, Susan E. Johnston, Anna W. Santure, and  
847 Carole M. Smadja. 2017. "Variation in recombination frequency and distribution across  
848 eukaryotes: Patterns and processes." *Philosophical Transactions of the Royal Society  
849 B: Biological Sciences* 372 (1736). <https://doi.org/10.1098/rstb.2016.0455>.

850 Todesco, Marco, Gregory L. Owens, Natalia Bercovich, Jean Sébastien Légaré,  
851 Shaghayegh Soudi, Dylan O. Burge, Kaichi Huang, et al. 2020. "Massive haplotypes

852 underlie ecotypic differentiation in sunflowers.” *Nature* 584 (7822): 602–7.  
853 <https://doi.org/10.1038/s41586-020-2467-6>.

854 Walsh, B., and M. Lynch. 2018. *Evolution and Selection of Quantitative Traits*. Oxford  
855 University Press. [https://global.oup.com/academic/product/evolution-and-selection-of-](https://global.oup.com/academic/product/evolution-and-selection-of-quantitative-traits-9780198830870?cc=ca&lang=en&)  
856 [quantitative-traits-9780198830870?cc=ca&lang=en&](https://global.oup.com/academic/product/evolution-and-selection-of-quantitative-traits-9780198830870?cc=ca&lang=en&).

857 Wang, Tongli, Andreas Hamann, Dave Spittlehouse, and Carlos Carroll. 2016. “Locally  
858 Downscaled and Spatially Customizable Climate Data for Historical and Future Periods  
859 for North America.” Edited by Inés Álvarez. *PLOS ONE* 11 (6): e0156720.  
860 <https://doi.org/10.1371/journal.pone.0156720>.

861 Weir, Bruce S, and C Clark Cockerham. 1984. “Estimating F-statistics for the analysis of  
862 population structure.” *Evolution* 38 (6): 1358–70.

863 Whitlock, M. C. 2005. “Combining probability from independent tests: the weighted Z-  
864 method is superior to Fisher’s approach.” *Journal of Evolutionary Biology* 18 (5): 1368–  
865 73. <https://doi.org/10.1111/j.1420-9101.2005.00917.x>.

866 Yeaman, Sam. 2013. “Genomic rearrangements and the evolution of clusters of locally  
867 adaptive loci.” *Proceedings of the National Academy of Sciences of the United States of*  
868 *America* 110 (19): E1743–E1751. <https://doi.org/10.1073/pnas.1219381110>.

869 Yeaman, Sam, Aleeza C. Gerstein, Kathryn A. Hodgins, and Michael C. Whitlock. 2018.  
870 “Quantifying how constraints limit the diversity of viable routes to adaptation.” *PLoS*  
871 *Genetics* 14 (10): e1007717. <https://doi.org/10.1371/journal.pgen.1007717>.

872 Yeaman, Sam, Kathryn A. Hodgins, Katie E. Lotterhos, Haktan Suren, Simon Nadeau,  
873 Jon C. Degner, Kristin A. Nurkowski, et al. 2016. “Convergent local adaptation to  
874 climate in distantly related conifers.” *Science* 353 (6306): 1431–3.  
875 <https://doi.org/10.1126/science.aaf7812>.

876 Zhou, Xiang, Peter Carbonetto, and Matthew Stephens. 2013. “Polygenic Modeling with  
877 Bayesian Sparse Linear Mixed Models.” *PLoS Genetics* 9 (2): 1003264.  
878 <https://doi.org/10.1371/journal.pgen.1003264>.

879  
880  
881

## Appendix

### Parametrizing simulations of local adaptation

Consider a hypothetical species of conifer inhabiting British Columbia, Canada. There may be many hundreds of millions of individuals in this hypothetical species distributed across the landscape. It would be computationally intractable to simulate all individuals forward-in-time incorporating adaptation to environmental variation across the landscape with recombining chromosomes, even with modern population genetic simulators. In our simulations we scaled several population genetic parameters to model a large population when simulating a much smaller one. In the following sections, we outline and justify the approach we used to scale pertinent population genetic parameters.

#### Mutation rate

We set the neutral mutation rate such that there would be an average of around 20 SNPs in each gene with a minor allele frequency threshold greater than 0.05. This number was motivated by the average number of SNPs per gene in the lodgepole pine dataset described by (Yeaman et al. 2016). We found that a neutral mutation rate ( $\mu_{neu}$ ) of  $10^{-8}$  in our simulations achieved an average of 23.3. Note that this  $\mu_{neu}$  gave a very low population-mutation rate within demes,  $4N_d\mu_{neu} = 4.0 \times 10^{-8}$ .

There are no estimates available of the mutation rate for locally adaptive alleles. As such, we had no empirical estimates to base our simulations on. Instead, we opted to use mutation rates that resulted in multiple locally beneficial alleles establishing in our simulations. For directional selection, we found that a mutation rate of  $\mu_{alpha} = 3 \times 10^{-7}$  resulted in an average of 6.XX locally adaptive genes establishing. For stabilizing selection, a mutation rate of  $\mu_{alpha} = 1 \times 10^{-8}$ , resulted in similar numbers of genes establishing. Note that in our model of directional selection, only a single nucleotide in each of 12 genes could mutate to a locally beneficial allele. In the case of stabilizing selection, all 1,000bp in the simulated gene could give rise to mutations that affected phenotype.

#### Recombination rates

We based our choice of recombination rate on patterns of LD decay reported for conifers. The pattern of LD decay in a panmictic population can be predicted by the population-scaled recombination parameter ( $\rho = 4N_e r$ ; Charlesworth and Charlesworth 2010), but the pattern of LD decay in structured populations is less well described. In conifers, LD decays very rapidly in conifers and  $\rho \approx 0.005$  has been estimated (Pavy et al. 2012). However, per basepair recombination rates ( $r$ ) in conifers are extremely low, estimated to be on the order of 0.05 cM/Mbp - more than 10× lower than the average for humans (Stapley et al. 2017). This implies a very large effective population size of



roughly  $\frac{0.005}{4 \times 0.5 \times 10^{-8}} = 2.5 \times 10^6$ , much larger than is feasible to simulate. To achieve a similar number of recombination events through time in our simulated populations, we needed to increase  $r$  above what has been empirically estimated. We chose a recombination rate that gave us a pattern of LD decay that was similar to what has been observed in conifers. We found that a per base pair recombination  $r = 1 \times 10^{-7}$  (i.e. roughly  $200 \times$  greater than in natural populations) gave a pattern of LD in our simulated populations that was similar to what has been reported for conifers.

## Selection coefficients

It is difficult to choose a realistic set of selection parameters for modelling local adaptation because there are, at present, no estimates of the distribution of fitness effects for mutations that have spatially divergent effects. However, common garden studies of a variety of taxa have estimated fitness differences of up to 35-45% between populations grown in home-like conditions versus away-like conditions (Hereford 2009; Bontrager et al. 2020). Motivated by such studies, we chose to parametrize selection using the fitness difference between home versus away environments.

When modelling directional selection, our simulations contained 12 loci that could mutate to generate a locally beneficial allele. The phenotypic optima that we simulated ranged from -7 to 7 and we modelled selection on a locus as  $1 + s_a\theta$  for a homozygote and  $1 + hs_a\theta$  for a heterozygote, where  $s_a$  is the selection coefficient,  $\theta$  is the phenotypic optimum and  $h$  is the dominance coefficient. With a selection coefficient of  $s_a = 0.003$ , the maximum relative fitness was  $(1 + 7 \times s_a)^{12} = 1.28$  for an individual homozygous for all locally beneficial alleles. An individual homozygous for those alleles, but in the oppositely selected environment (i.e. present in the wrong deme) had a fitness of  $(1 - 7 \times s_a)^{12} = 0.775$ . Thus, there would be approximately 40% difference in fitness between well locally adapted individuals at home versus away in the most extreme case.

As stated the main text, for stabilizing selection simulations we chose  $V_s = 192$  as this gave a maximum of 50% difference in fitness between individuals grown in home-like conditions versus away-like conditions.

## Migration rate

We wanted to model populations with  $F_{ST}$  across the metapopulation of approximately 0.05, as has been reported for widely distributed conifer species such as lodgepole pine and interior spruce (Yeaman et al. 2016). For the stepping-stone simulations, we chose a migration rate of  $\frac{7.5}{2N_d}$  as we found that this gave a mean  $F_{ST}$  of 0.04. For an island model, we used the analytical formulae given in the main text to set  $m$  to achieve a mean  $F_{ST}$  of 0.03.

**Table S1** Population genetic parameters of a hypothetical organism, and how they are scaled in the simulations. The meta-population inhabits a  $14 \times 14$  2-dimensional stepping stone. Parameters are shown for a population with 12 loci subject to directional selection.

Parameter	Hypothetical Biological Value	Scaled Parameter	Unscaled (Simulation)
Global population size ( $N_e$ )	$10^6$	-	19,600
Number of demes ( $d$ )	196	-	196
Local population size ( $N_d$ )	5,100	-	100
Recombination rate ( $r$ )	$2.00 \times 10^{-9}$	$4N_d r = 0.00004$	$1 \times 10^{-7}$
Selection coefficient ( $s_a$ )	0.0001	$2N_d s_a = 0.6$	0.003
Migration rate ( $m$ )	$7.35 \times 10^{-4}$	$2N_d m = 7.5$	0.0375
Neutral mutation rate ( $\mu_{neu}$ )	$2 \times 10^{-10}$	$4N_e \mu_{neu} = 0.000004$	$10^{-8}$
Functional mutation rate ( $\mu_\alpha$ )	$2 \times 10^{-9}$	$4N_e \mu_\alpha = 0.00004$	$3 \times 10^{-7}$

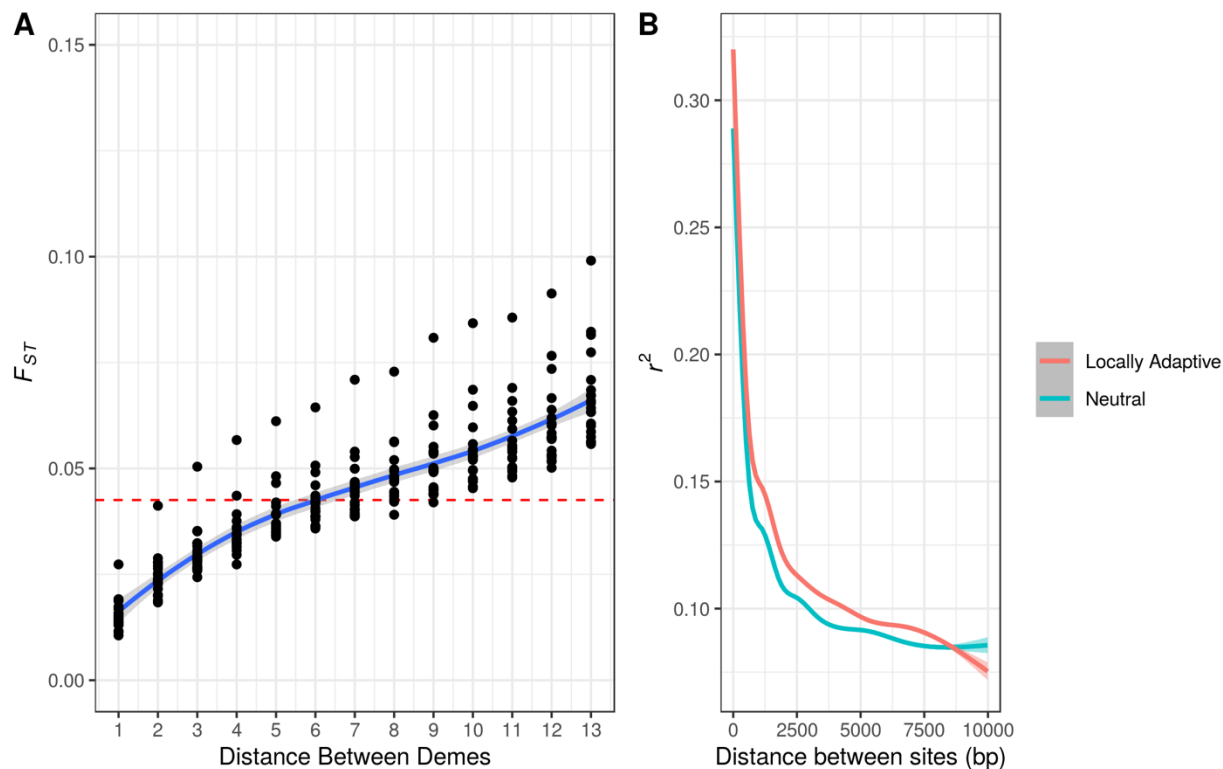


**Figure S1** Summary statistics from neutral simulations. A)  $F_{ST}$  between pairs of demes in stepping-stone populations. The average across replicates is 0.042. B) LOESS smoothed LD, as measured by  $r^2$ , between pairs of SNPs in genes that are either evolving neutrally or locally adaptation as indicated by the color. Smoothing was performed using the ggplot2 package in R.

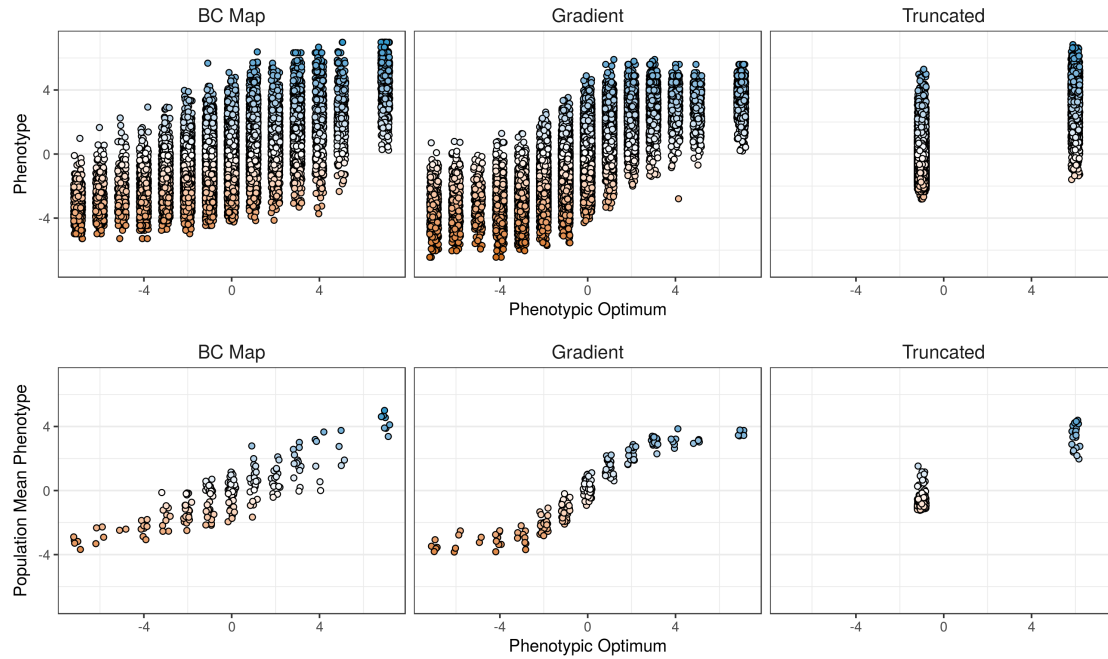


**Figure S2** Individual and population mean phenotypes observed in representative simulations for each of the environment maps simulated. A small amount of horizontal jitter was added to points for visualization purposes. Colors are for visualization purposes only.

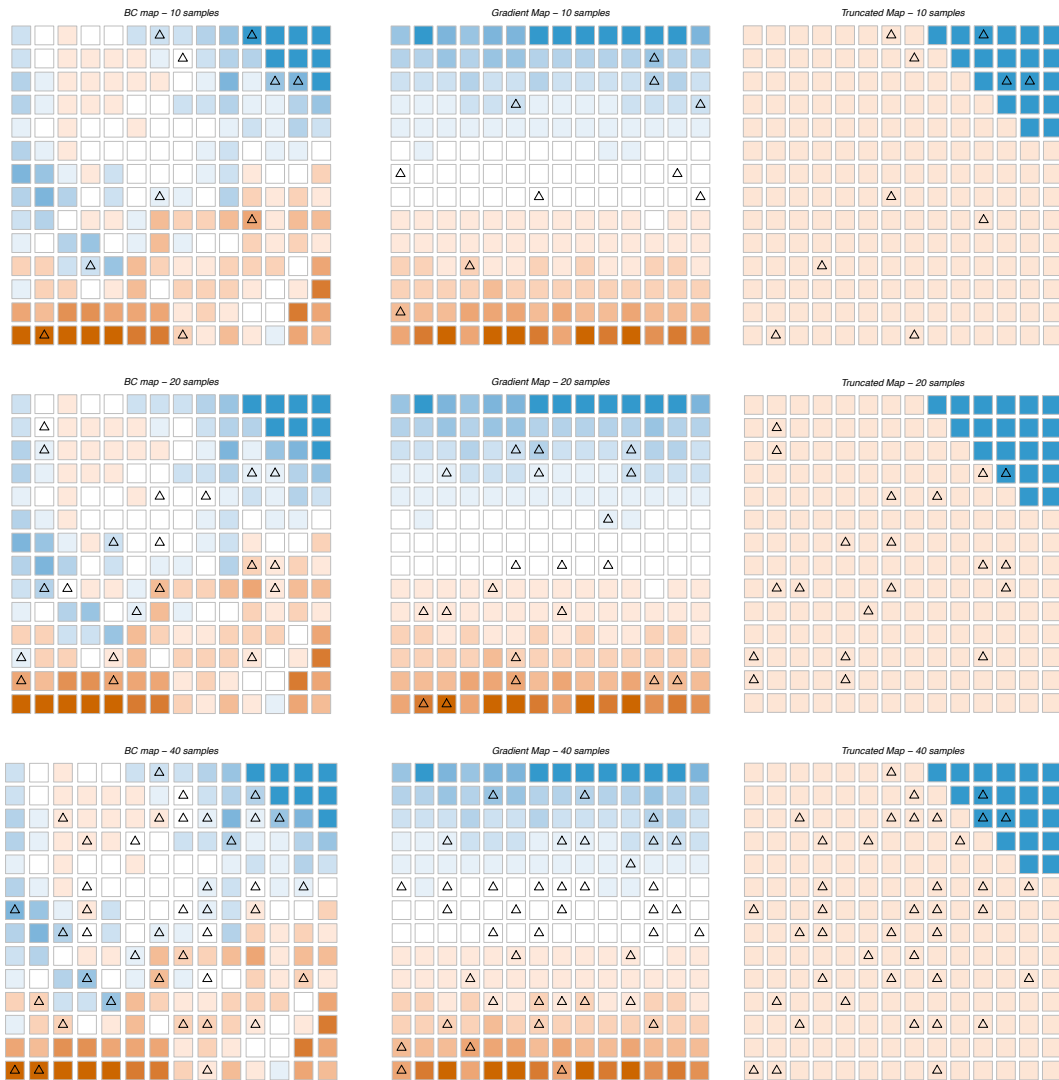


**Figure S3** Locations of sampled demes on the maps of environmental variation we assumed in the simulations. Triangles indicate the locations where individuals were sampled in each case. Colors represent the optimal phenotype in each population the same as Figure 1 in the main text.

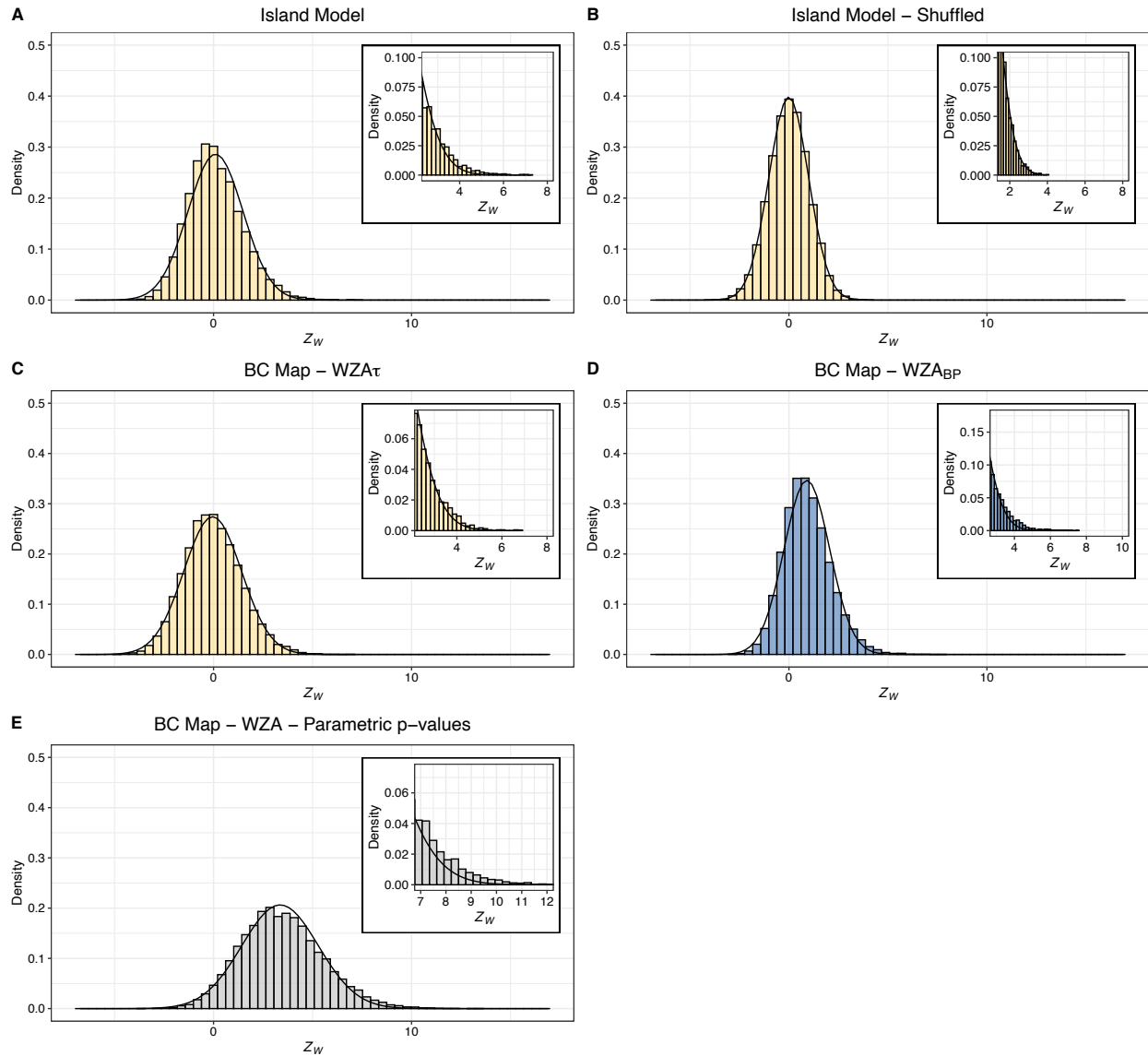


**Figure S4** The distribution of WZA scores from neutral simulations with details of the right tail in the insets. Overlaid on each panel is the normal distribution fitted to each dataset. In all cases, results from 20 simulation replicates are plotted together.

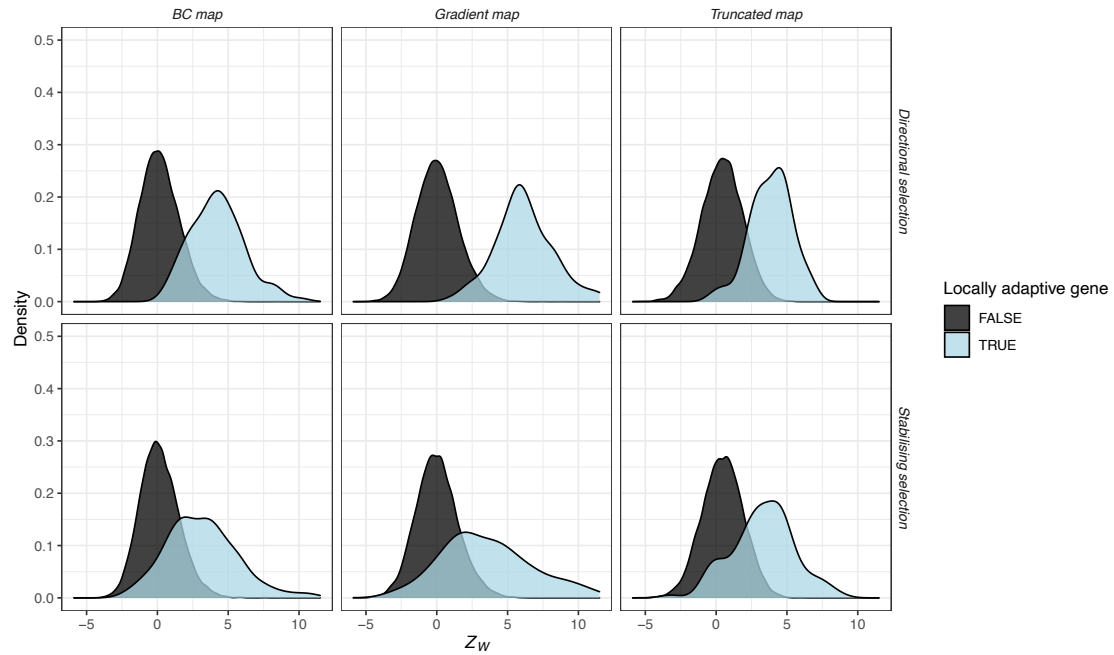


**Figure S5** The distribution of WZA scores from simulations of local adaptation. Note, the plot does not indicate the relative frequency of genes that are or are not locally adaptive.

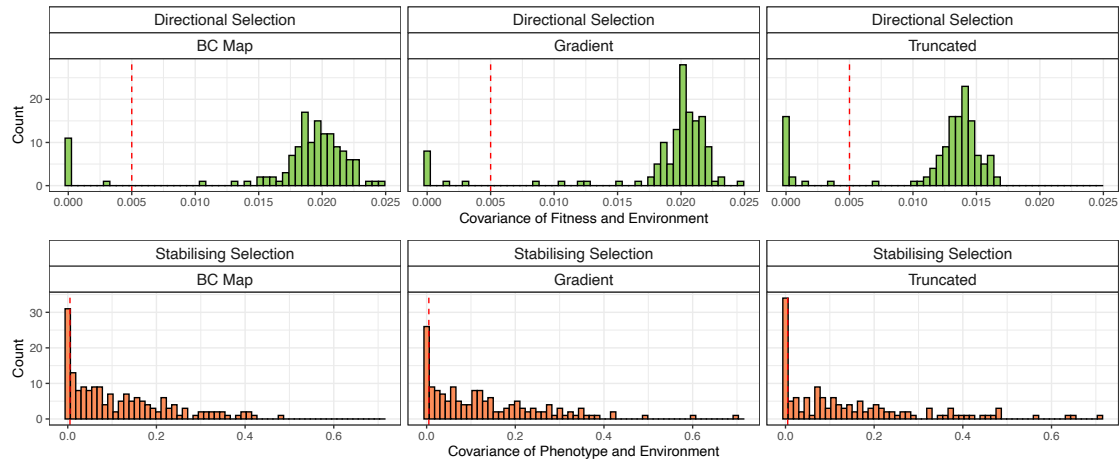


**Figure S6** The effect size distribution from simulations of local adaptation. The vertical line indicates the threshold we applied to the simulated data to classify genes as locally adaptive or not.



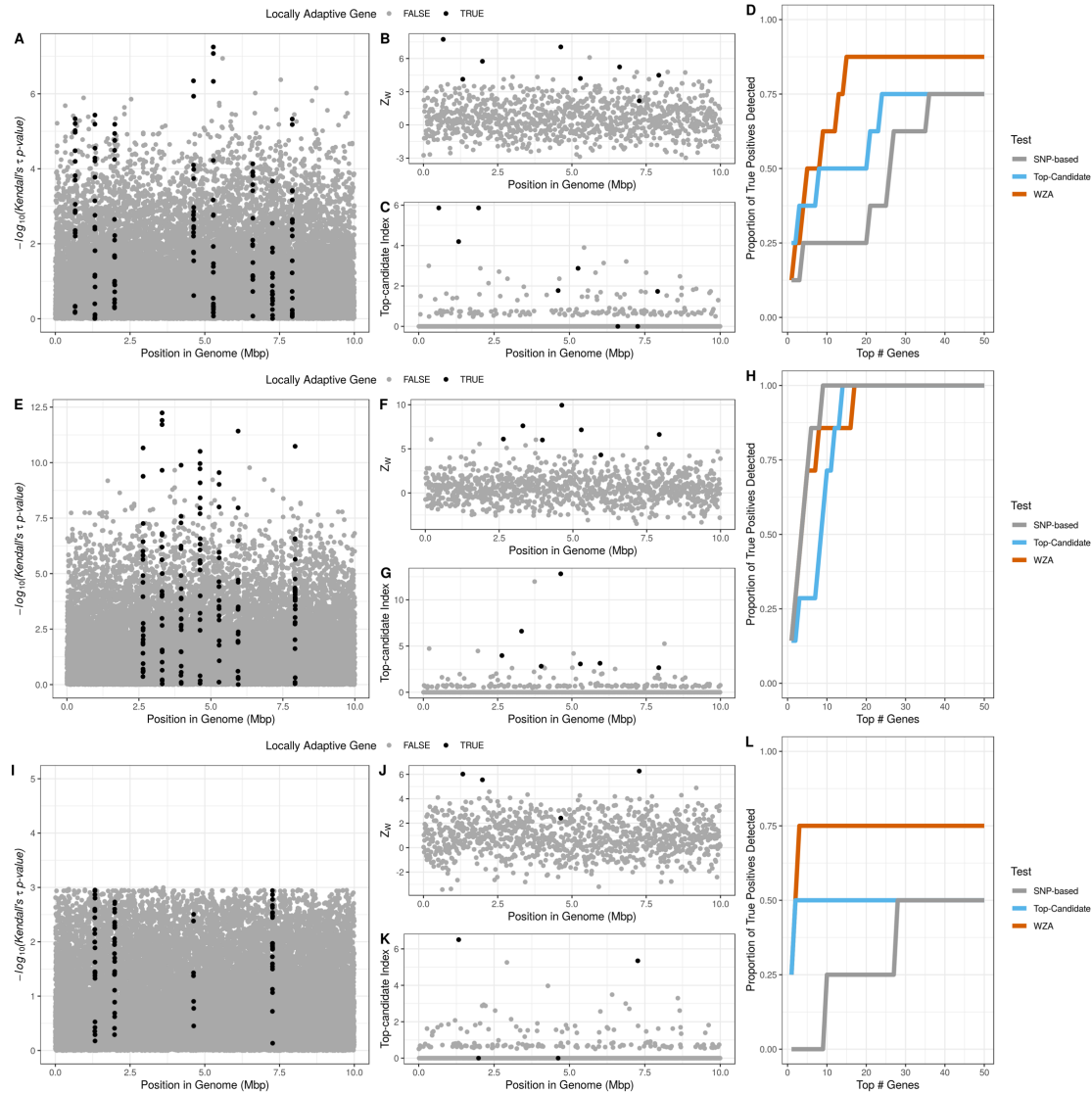


**Figure S7** Plots demonstrating the genomic landscape of genotype-environment correlations for a single replicate for each of the three maps of environmental variation we simulated. From top to bottom, the three rows correspond to the *BC Map* (panels A-D), the gradient map (panels E-H) and the truncated map (panels I-L), respectively. The leftmost panel in each row shows the Manhattan plot of  $-\log_{10}(\text{p-values})$  from Kendall's  $\tau$  (panels A, E and I). The central panels in each row show the distribution of  $Z_W$  scores from the WZA across the genome (B, F and J) and the distribution of results from the top-candidate method (C, G and K). The rightmost panels show the proportion of locally adapted genes identified using the three different tests for an increasing number of genes in the search effort. Results are shown for directional selection simulations. Note that only SNPs with a minor allele frequency  $> 0.05$  are shown in panels (A, E and I).

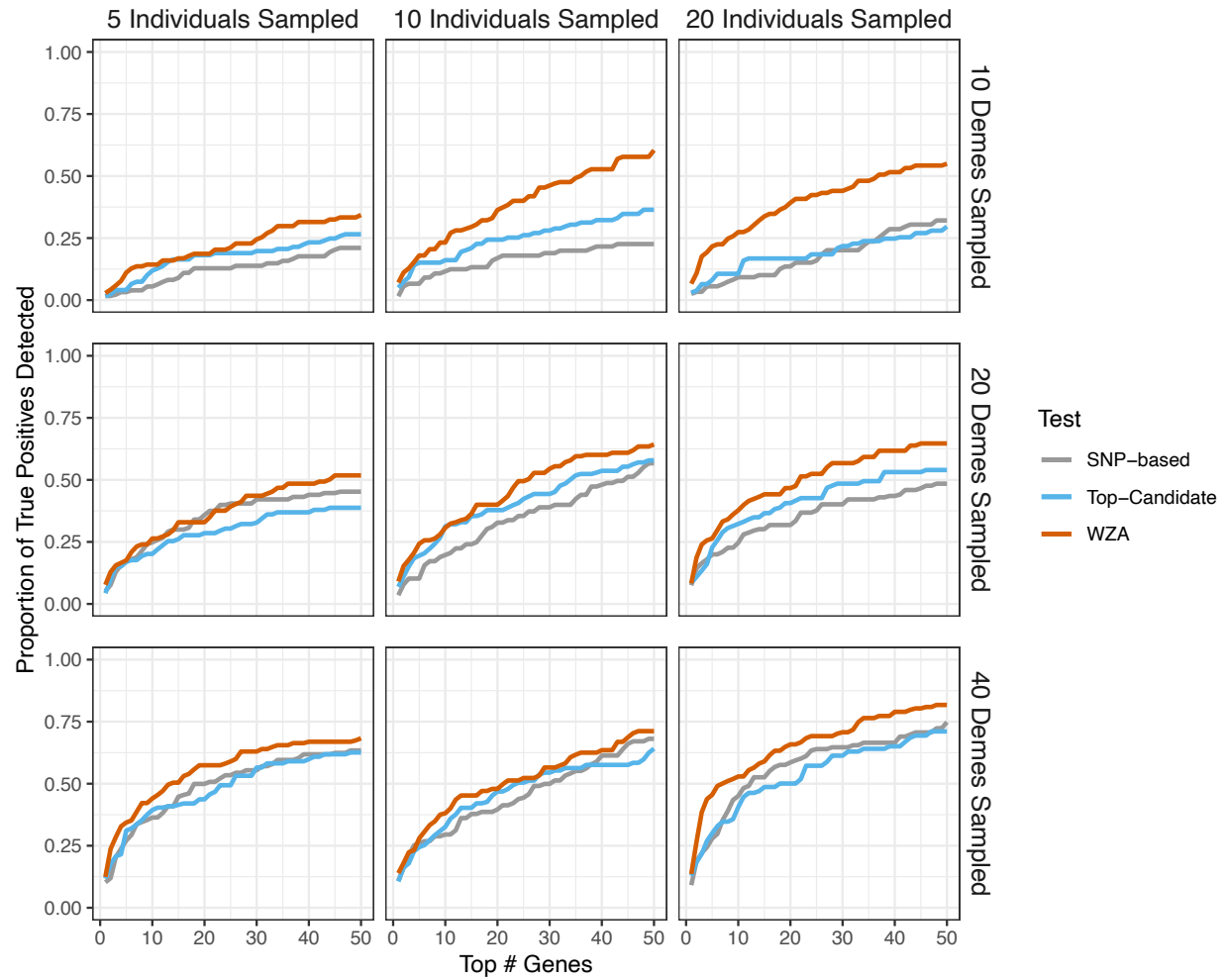


**Figure S8** Comparison of the WZA, the top-candidate and the single-SNP approaches with varying numbers of individuals sampled per deme. Simulations shown used the *BC map* and directional selection. Lines represent the mean of 20 simulation replicates.

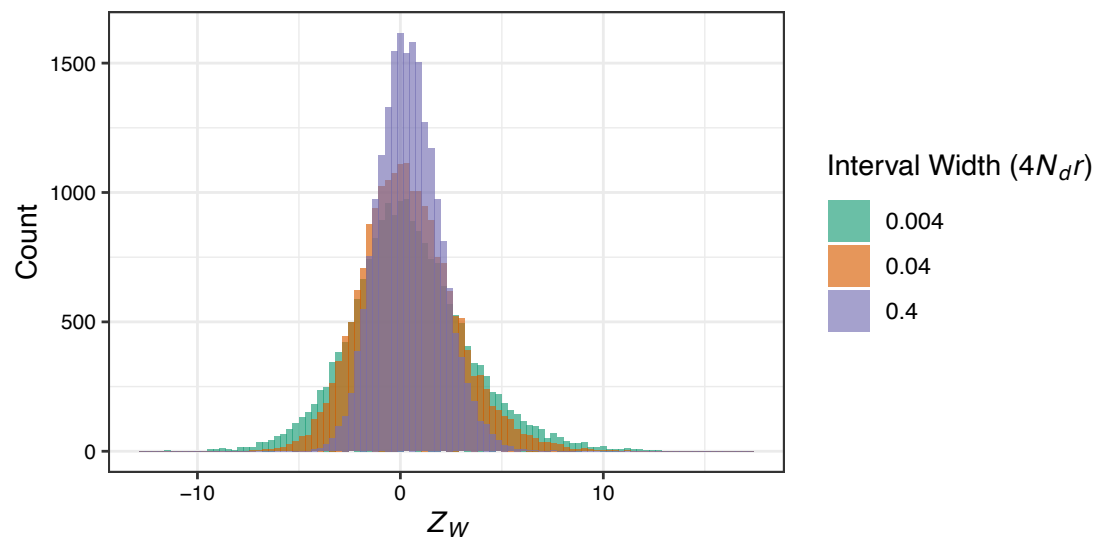


**Figure S9** The distribution of  $Z_W$  scores under different recombination rates.

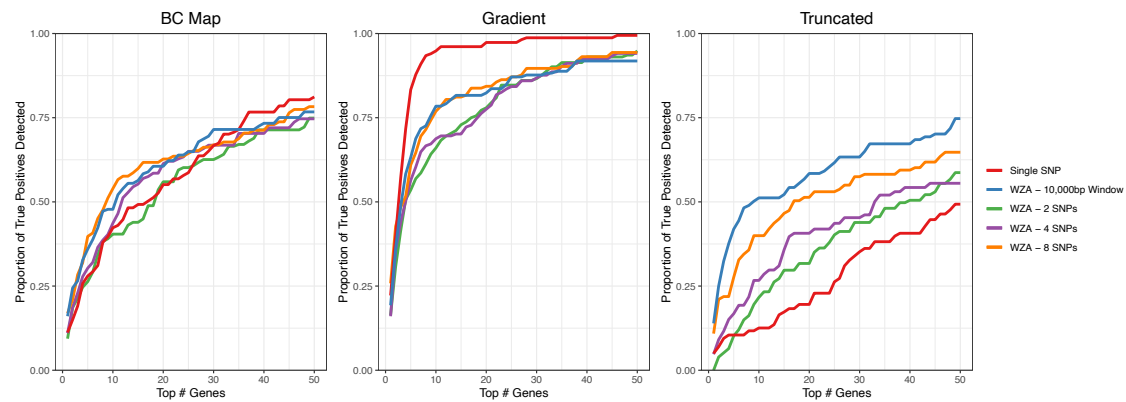


**Figure S10** Comparing the performance of the WZA genes identified using the WZA, using analysis windows analyzing a fixed number of SNPs. Lines represent the means of 20 replicates.

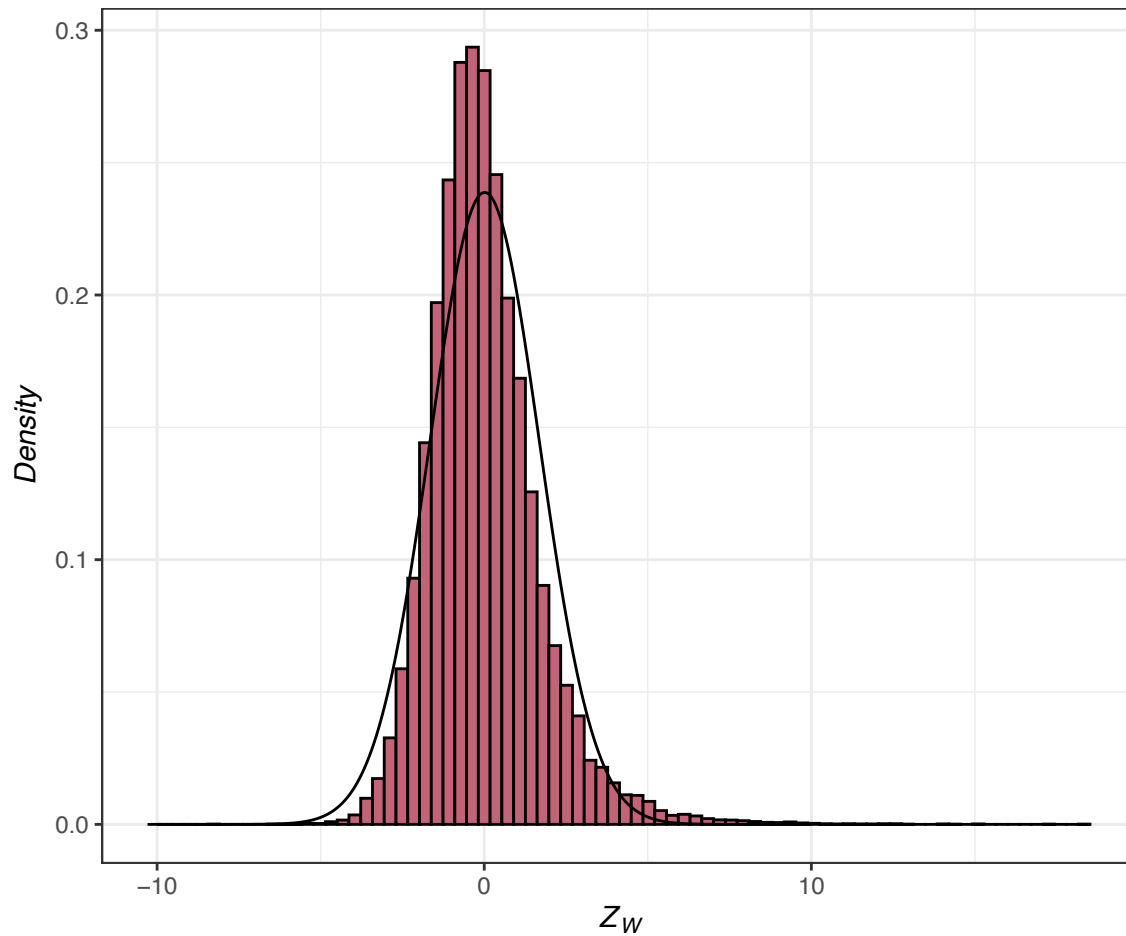


**Figure S11** The distribution of A) degree days < 0 (DD0) across the populations of P. contorta sampled by Yeaman et al (2016) and B)  $Z_W$  scores for the GEA on DD0. Note that the DD0 values in A) are unscaled. In B) the curve shows a normal distribution fitted to the data.

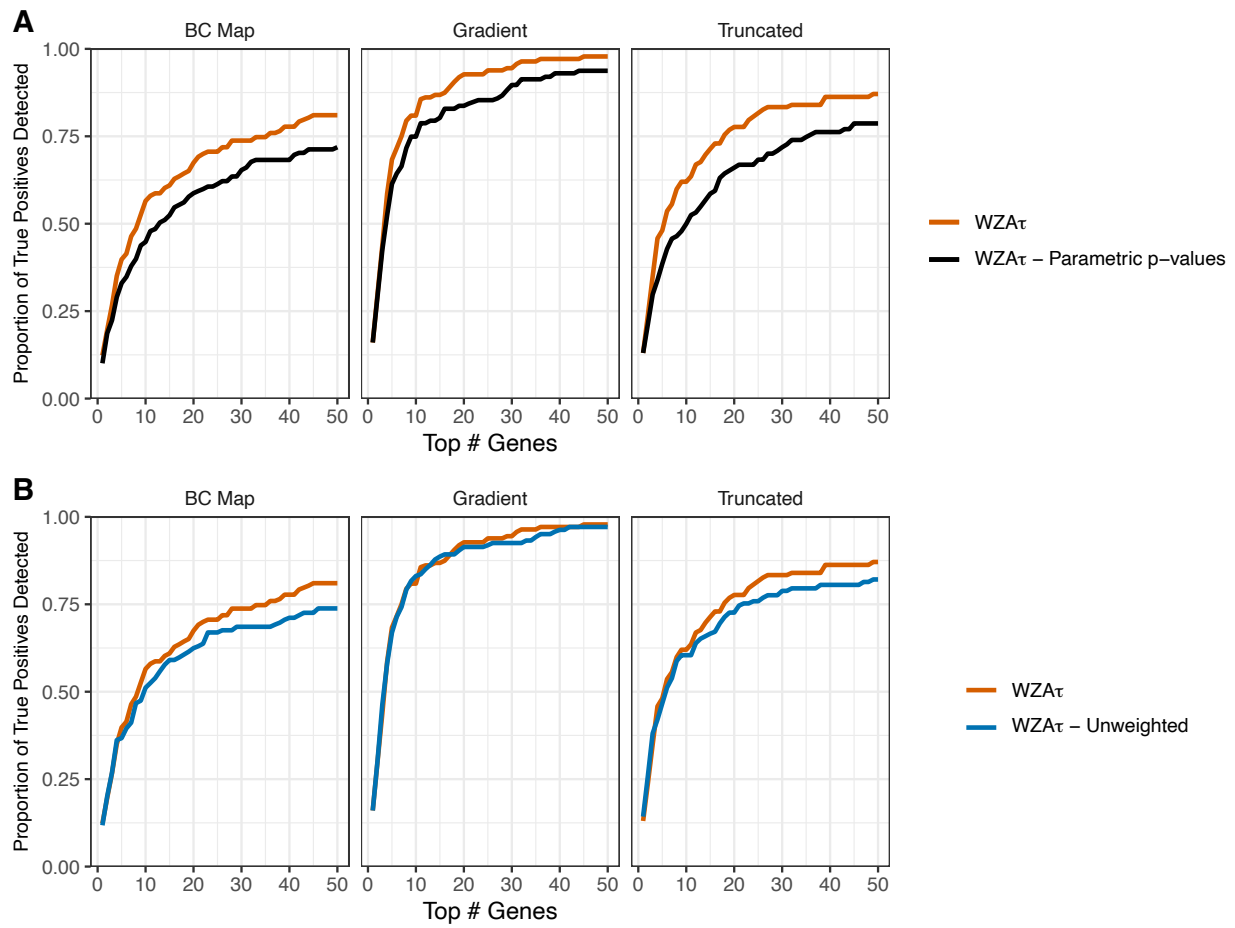


**Figure S12**

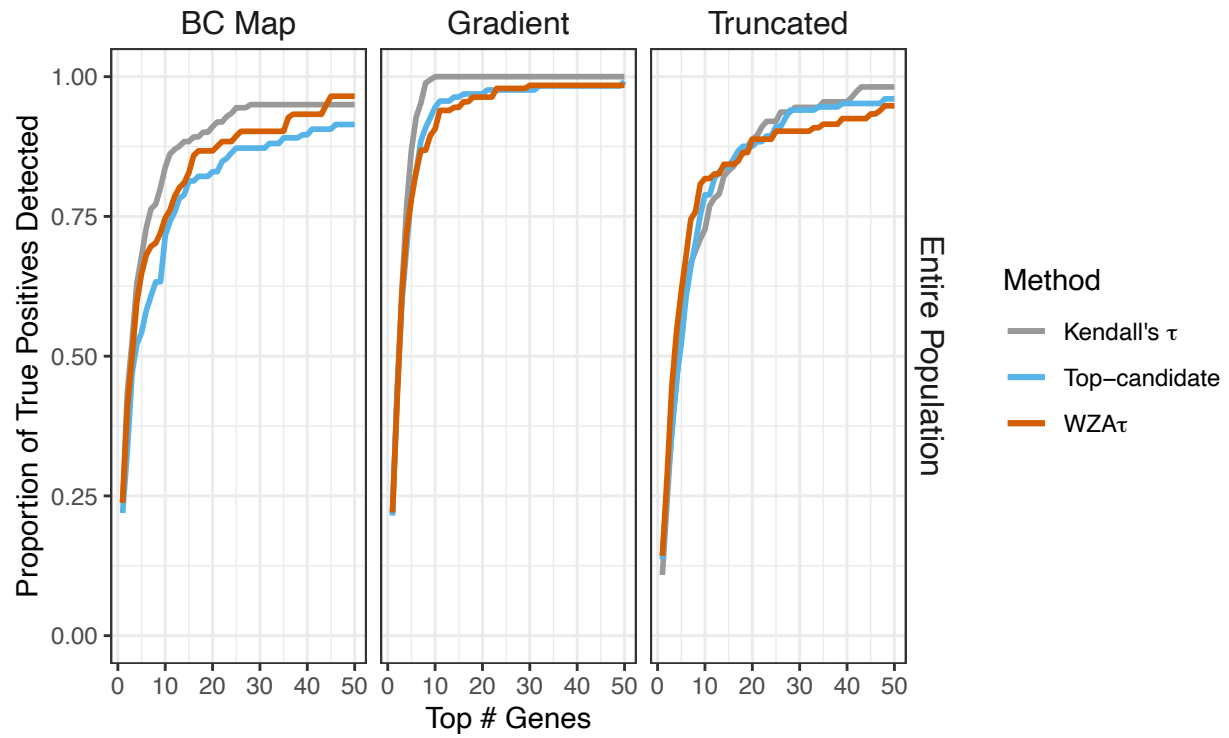


**Figure S13** A comparison of three methods to identify the genetic basis of local adaptation when one has complete information on all aspects of the metapopulation.